Università degli Studi di Padova

Scuola di Scienze
Dipartimento di Fisica e Astronomia
"Galileo Galilei"

Tesi di Laurea Magistrale in Fisica

RADIATIVE CORRECTIONS TO THE ELASTIC SCATTERING OF MUONS ON ELECTRONS

Candidato:

MARCO ROCCO
Matricola 1132679

Relatore:

Dott. MASSIMO PASSERA
Istituto Nazionale di Fisica Nucleare
Sezione di Padova

Anno Accademico 2016 – 2017

ABSTRACT

In this thesis the Standard Model theoretical prediction for the elastic scattering of muons on electrons is analyzed. In particular, we focus on the calculation of the radiative corrections at next-to-leading order in QED, which turn out to be in agreement with the most recent result in literature. Moreover, we discuss the application of this theoretical prediction in the framework of a new proposal, which aims to compute the leading-order hadronic contribution to the muon anomalous magnetic moment within an improved accuracy.

CONTENTS

1

INTRODUCTION

Aim of this thesis is the calculation of the Standard Model theoretical prediction for the scattering amplitude of the elastic process $\mu\, e \to \mu\, e$ at next-to-leading order (NLO) in QED.

It is a fact widely acknowledged, that a long-standing discrepancy between the experimental value of the muon anomalous magnetic moment a_μ and the Standard Model (SM) prediction exists (1), (2), (3), (4), (5). From the most recent data we get (3)

$$a_\mu^{\text{exp}} - a_\mu^{\text{SM}} = 249\,(87) \cdot 10^{-11}\,,$$

a discrepancy which may indicate new physics beyond the SM (6).

The main limit on the SM theoretical prediction for a_μ, treated in chapter 2, is the accuracy resulting from the computation of the leading order hadronic (HLO) contribution, namely the difficulty in considering strong interactions effects, which cannot be treated perturbatively at low energies. In fact, the hadronic uncertainty dominates that of the SM prediction and it is comparable with the experimental one. Currently, apart from lattice Quantum Chromodynamics (QCD) results (7), (8) — which are not yet competitive, there is one general approach to this issue, based on analiticity and unitarity of Feynman amplitudes.

A new approach has been proposed recently (9). It is possible to calculate the HLO contribution to a_μ via measurements of the effective electromagnetic coupling $\alpha(q^2)$, with q^2 the squared 4-momentum transfer, in a space-like region where q^2 is negative. In fact, one extracts the hadronic contribution to $\Delta\alpha(t)$, where t is a Mandelstam space-like variable, by subtracting the leptonic contribution, calculable order-by-order in perturbation theory.

According to that second approach, a particular process — μ-e elastic scattering in a fixed-target experiment — has been chosen to determine a_μ^{HLO} (10). Since the process occurs as a $t-$channel, the running of α is measured in a space-like region and the hadronic part $\Delta\alpha_{\text{had}}(t)$ is extracted from the comparison of the experimental data with the SM prediction at Next-to-Next-to-Leading Order (NNLO). Aim of this proposal, whose name is MUonE, is to obtain a result with an accuracy comparable to the goal of future a_μ measurements

at Fermilab (11) and J-PARC (12), i.e. 0.14 parts per million or better.

This explains why the calculation of the SM theoretical prediction for the differential cross section of the elastic process $\mu\, e \to \mu\, e$ at NLO is the subject of this thesis. Particularly, the calculation is treated in chapter 3 and this result happens to be the first crucial step, from a theoretical viewpoint, within the framework of the MUonE proposal. Also, we checked the result for the same differential cross section obtained earlier in the literature. As we will see, our results agree with the latest one, while some of the pioneering publications contain typos or errors.

Our calculation has been carried out either by hand or by use of `FeynCalc`, a `Mathematica` package for symbolic evaluation of Feynman diagrams and algebraic calculations in quantum field theory and elementary particle physics (13)-(14).

Conclusions are drawn in chapter 4.

2

MUON $g-2$

It is a fact widely acknowledged, that the Standard Model (SM) of elementary particles, as a relativistic quantum field theory, provides surprisingly accurate predictions in the High Energy Physics framework. Also, several tests have been performed, searching for possible SM violations, and one of the most stringent of them is the comparison between the theoretical prediction for lepton magnetic moments and their experimentally measured values.

2.1 A (VERY) BRIEF HISTORICAL NOTE

Among the different properties a lepton has – like charge, spin, mass and lifetime – there are the so called magnetic and electric dipole moments, which are interesting both from a classical and a quantum viewpoint. As it is known, for what concerns the magnetic case, dipole moments may arise classically from electrical currents. For example, an orbiting particle of charge q, mass m and orbital angular momentum $\vec{L} = m\vec{r} \times \vec{v}$ shows a magnetic dipole moment

$$\vec{\mu}_L = \frac{q}{2m}\vec{L}\,, \tag{2.1}$$

where $\vec{r}$ and $\vec{v}$ are the position and the velocity of the particle.

Also, if we define a spin operator $\mathbf{S} = \sigma/2$, which replaces the angular momentum operator $\mathbf{L}$ in a generalised form of (2.1), one may write

$$\mu_S = g\left(\frac{Q}{2m}\right)\frac{\sigma}{2}\,, \tag{2.2}$$

where σ_i are the Pauli matrices ($i = 1, 2, 3$), $Q = -e$ for charged leptons, $Q = +e$ for charged antileptons and g is defined as the gyromagnetic ratio.

Historically, the first approach to predict or measure g was that of Goudschmidt and Uhlenbeck (*15*) in 1925. They postulated an intrinsic angular momentum of $\hbar/2$ for the electron, associated to a magnetic dipole moment equal to $e\hbar/2mc$, while the classical prediction was $g = 1$. From an experimental viewpoint, in the same period, Back and Landé (*16*) carried out several studies based on the Zeeman effect to verify this statement. Nevertheless, they did not manage to

really determine g.

In 1928, one year after Pauli (17) left g as a free parameter in his quantum mechanical treatment of the electron spin, Dirac (18) presented his relativistic quantum field theory, which predicted $g = 2$. This was soon confirmed by some experimental results (e.g. Kinsler and Houston (19) in 1934), although relatively large experimental errors were also included.

It was not until 1947, at the famous Shelter Island conference, that experiments finally suggested or showed that the electron magnetic moment actually exceeded 2 by about 0.12%, as Kusch and Foley (20) found out in 1948 with $g_e = 2.00238(10)$. This was the first indication of the existence of an "anomalous" magnetic moment

$$a_\ell \equiv \frac{g_\ell - 2}{2} \quad (\ell = e, \mu, \tau). \tag{2.3}$$

The next year, Schwinger (21) obtained his celebrated result[1] for the leading order (LO) radiative correction to a_e:

$$a_\ell^{\text{QED (LO)}} = \frac{\alpha}{2\pi}, \tag{2.4}$$

also putting an end to the problems which Quantum Electrodynamics (QED) was suffering from in the Thirties.[2] In fact, it was incapable of making quantitative predictions at orders higher than the tree level and Dirac used to write that, "because of its extreme complexity, most physicists will be glad to see the end of it" (22).

As a result, these experiments and calculations provided one of the first tests of the virtual, or radiative, quantum corrections predicted by a relativistic quantum field theory.

2.2 THE ANOMALOUS MAGNETIC MOMENT OF THE MUON

Since then, either the evaluation of the SM prediction for the lepton anomalous magnetic moments or their experimental measurements have occupied numerous researches for over sixty years.

If, on one hand, the agreement of the QED prediction for a_e with the experimental results provided one of the early confirmation of this theory – and nowadays represents one of the most precisely measured quantities in particle physics, it is also true that a_e itself is quite insensitive to strong and weak interactions and to yet unknown Beyond SM (BSM) physics, especially at higher energy scales.

On the other hand, the long-standing discrepancy of 3-4 standard deviations between the theoretical prediction for a_μ and its measurements may be a more useful tool to uncover BSM physics effects.

1 The same result will be obtained in subsection 2.3.1 with a different technique.

2 Of course, Schwinger found the result for the electron case, but, as it can be noticed, the contribution is universal for all charged leptons and (2.4) has been generalized by bearing that in mind.

In fact, for a lepton ℓ, the contribution to a_ℓ is generally proportional to m_ℓ^2/Λ^2, where m_ℓ is the mass of the charged lepton and Λ the energy scale at which BSM effects show up. It is clear now that a factor of $(m_\mu/m_e)^2 \sim 4 \cdot 10^4$ enhances the sensitivity in the muon case.[3]

In this chapter we will briefly review the SM calculation for the muon anomalous magnetic moment, a_μ^{SM}. A more interested reader can find a more detailed analysis in (1), (2), (3), (4), (5).

Particularly, we are considering the three contributions into which a_μ^{SM} is usually split: QED, electroweak (EW) and hadronic. They are respectively discussed in sections 2.3, 2.4 and 2.5.

2.3 QED CONTRIBUTION TO a_μ

The pure QED contribution to the anomalous magnetic moment, coming from the interaction of the charged leptons e, μ and τ with the photon, is by far the largest. Then, as a dimensionless quantity, a_μ may be represented as an expansion in powers of α, where the coefficients depend on the mass ratios of the three leptons.

Generally speaking, we can cast a_μ in the following form:

$$a_\mu^{\text{QED}} = A_1 + A_2\left(\frac{m_\mu}{m_e}\right) + A_2\left(\frac{m_\mu}{m_\tau}\right) + A_3\left(\frac{m_\mu}{m_e}, \frac{m_\mu}{m_\tau}\right), \tag{2.5}$$

where m_e, m_μ and m_τ are the electron, muon and tau masses, respectively. Since QED is a renormalizable theory, we can expand the A_i functions ($i = 1, 2, 3$) as a power series in α/π and compute them order-by-order:

$$A_i = A_i^{(2)}\left(\frac{\alpha}{\pi}\right) + A_i^{(4)}\left(\frac{\alpha}{\pi}\right)^2 + A_i^{(6)}\left(\frac{\alpha}{\pi}\right)^3 + \dots . \tag{2.6}$$

The term A_1, which takes into account the QED Feynman diagrams containing no electrons or taus as external legs, is mass independent (then, universal for all lepton magnetic moments).

The term A_2 is characterized by one mass scale ($m_\mu/m_{e,\tau}$) and therefore it becomes different from zero if an additional lepton loop, of a lepton which is not a muon, is present. This leads to two loops at least ($A_2^{(2)} = 0$) and there are two possibilities: an electron loop which contributes to $A_2(m_\mu/m_e)$ and shows up as a large effect term $\propto \log\left(m_\mu^2/m_e^2\right)$ or a tau loop which contributes to $A_2(m_\mu/m_\tau)$ and shows up as a small effect term $\propto \log\left(m_\mu^2/m_\tau^2\right)$.

Finally, a similar discussion leads to $A_3^{(2)} = A_3^{(4)} = 0$.

3 The lepton τ, although way heavier than the μ, is not considered since the very short lifetime of the former makes it difficult to reach enough sensitivity in such measurements (23).

2.3.1 *One-loop contribution*

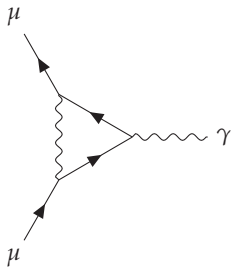

Only one diagram shows up in the evaluation of the order α contribution to a_μ. It is drawn aside and yields the above mentioned result by Schwinger: $A_1^{(2)} = 1/2$.

Hereafter, it will be obtained by the projection technique, but first we have to recall some features about the Lorentz structure of the QED minimal vertex, that is the 3-point function $-ie\Gamma^\mu \equiv \langle \overline{\psi} A^\mu \psi \rangle$, where ψ ($\overline{\psi} = \psi^+\gamma^0$) is the (barred) spinorial representation of the muon, A is the vectorial representation of the photon and e is the electric charge.

If we assign a 4-momentum p to the incoming muon, a 4-momentum p' to the outgoing one and we define the transferred 4-momentum $q \equiv p - p'$, a spinorial representation in the momentum space, $u(p)$ and $\overline{u}(p')$ respectively, will be associated to them.

Now, from the Lorentz structure of the 3-point function, one may write:

$$-ie\,\overline{u}(p')\Gamma^\mu u(p) = -ie\,\overline{u}(p')(a_1\gamma^\mu + a_2 p^\mu + a_3 p'^\mu)u(p)\,.$$

By recalling the Ward Identity, which holds in QED as

$$\overline{u}(p')q_\mu\Gamma^\mu u(p) = \overline{u}(p')(a_1 \not{q} + a_2\, q\cdot p + a_3\, q\cdot p')u(p) = 0$$

and by using $p^2 = p'^2 = m_\mu^2$ and the Dirac equation, it follows that $a_2 = a_3$. Therefore:

$$-ie\,\overline{u}(p')\Gamma^\mu u(p) = -ie\,\overline{u}(p')(a_1\gamma^\mu + a_2(p+p')^\mu)u(p)\,.$$

Now we may rewrite the 3-point correlator by using the Gordon identity,[4] eventually finding:

$$-ie\,\overline{u}(p')\Gamma^\mu u(p) = -ie\,\overline{u}(p')\Big(F_1(q^2)\gamma^\mu + F_2(q^2)\frac{i\sigma^{\mu\nu}}{2m_\mu}q_\nu\Big)u(p)\,, \quad (2.7)$$

where $\sigma^{\mu\nu} \equiv \frac{i}{2}[\gamma^\mu, \gamma^\nu]$ represents the spin $1/2$ angular momentum tensor, while F_1 and F_2 are the form factors, functions of the squared transferred momentum.

In the static limit, defined by $q \to 0$, one has:

$$F_1(0) = 1, \qquad F_2(0) = a_\mu\,, \quad (2.8)$$

where the first relation is usually called the charge renormalization condition (in units of the physical charge e, which was taken out in (2.7) by definition), while the second is the finite prediction for a_μ.

4 $\overline{u}(p')\gamma^\mu u(p) = \overline{u}(p')\Big(\frac{(p+p')^\mu}{2m_\mu} + i\sigma^{\mu\nu}\frac{(p-p')_\nu}{2m_\mu}\Big)u(p)$.

In fact, we may infer from (2.7) that the interaction of a spin 1/2 particle, like the muon, with an initial spin state s and a final one s', with a (static) external magnetic field, represented by $A^\mu_{\text{ext}} = (0, \vec{A})$, is regulated via the interaction hamiltonian

$$H_{\text{mag}}(q^2) = \frac{e}{2m_\mu}\overline{u}(p',s')(F_1(q^2) + F_2(q^2))i\sigma^{i\nu}q_\nu A_{\text{ext,i}}\, u(p,s)\,. \tag{2.9}$$

Then, by use of (2.8), the quantum prescription $q_j \to -i\nabla_j$ and the following which hold in the static limit:

$$\overline{u}(0,s')\sigma^{i0}u(0,s) = 0, \quad \overline{u}(0,s')\sigma^k u(0,s) = 2\delta_{ss'}S^k\,,$$

where $\sigma^{\text{ij}} = \epsilon^{\text{ijk}}\sigma^k$ and $\mathbf{S}$ is the spin operator defined in section 2.1, one eventually obtains:

$$H_{\text{mag}}(0) = -\frac{e}{2m_\mu}[2(1+F_2(0))\epsilon_{\text{kji}}S_k\nabla_j A_{\text{ext,i}}]\,. \tag{2.10}$$

This last equation, by using the definition given in (2.2) and since a magnetic field operator $\mathbf{B}$ is equal to $\nabla \times \mathbf{A}$, we may write

$$H_{\text{mag}}(0) = -\mu_S \cdot \mathbf{B}\,, \tag{2.11}$$

where now

$$g_\mu = 2(1+F_2(0)) \quad \longleftrightarrow \quad F_2(0) = \frac{g_\mu - 2}{2} \equiv a_\mu\,,$$

which is what we claimed in (2.8).

Now, aiming to compute the leading order QED contribution to a_μ, we are going to extract $F_2(0)$ from the LO radiative corrections to the QED vertex by a projection technique.

Referring ourselves to the diagram aside, we may write the one-loop contribution to that correlator in d dimensions in order to regularize its UV divergence:

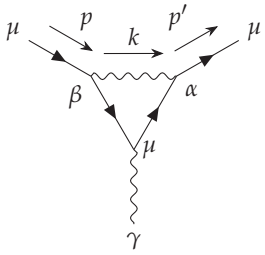

$$i\overline{u}'\Gamma^\mu u = -(e\mu^{\frac{\varepsilon}{2}})^3\int\frac{\mathrm{d}^d k}{2\pi^d}\frac{\gamma^\alpha(\not{p}' - \not{k} + M)\gamma^\mu(\not{p} - \not{k} + M)\gamma_\alpha}{[(p'-k)^2 - M^2][(p-k)^2 - M^2][k^2 - \lambda^2]}\,, \tag{2.12}$$

where μ is the 't Hooft dimensional parameter, $\varepsilon = 4 - d$, k is the loop momentum, λ is a fictitious mass for the photon, introduced to regularize IR divergences, $\overline{u}' \equiv \overline{u}(p')$, $u \equiv u(p)$ and $M \equiv m_\mu$; the iε prescription has been suppressed for brevity.

Before proceeding, it is useful to notice that, either in the UV domain or in the IR one, we may find that the integral diverges proportionally to γ^μ. This, along with QED strict renormalizability, explains why we should expect a finite contribution to $F_2(0)$, which is the form factor of the $\sigma^{\mu\nu}$ term.

On the other hand, we come back to the calculation with the introduction of two Feynman parameters,[5] y and z, leading to a denominator D of this shape:

$$D = [k^2 - 2k \cdot (p'y - pz) - \lambda^2(1-y-z) + (y+z)(p'^2 - M^2)]^3 \,,$$

which reduces to

$$D = [k^2 - 2k \cdot b - \lambda^2(1-y-z)]^3$$

if the incoming and outgoing muons are on-shell and if we define the 4-momentum $b^\mu \equiv yp'^\mu + zp^\mu$. We also make a standard shift for the loop momentum, $k^\mu \to k^\mu - b^\mu \equiv k^\mu$, which leaves invariant the measure and lets the integral become

$$i\overline{u}'\Gamma^\mu u = -(e\mu^{\frac{\varepsilon}{2}})^3\Gamma(3)\int_0^1 \mathrm{d}y \int_0^{1-y} \mathrm{d}z \int \frac{\mathrm{d}^d k}{2\pi^d} \frac{N^\mu(p',p,k)}{[k^2-C]^3} \,, \qquad (2.13)$$

where $C \equiv \lambda^2(1-y-z) + (yp'+zp)^2$ is a function which does not depend on the loop momentum and $N^\mu(p',p,k)$ is the numerator modified by the shift. This latter may be split into three contributions:

- N_0^μ, constant in the loop momentum k, whose k-integral yields a finite contributions to Γ^μ;
- N_1^μ, linear in k, whose k-integral is null by parity considerations: we integrate an odd function over an even domain;
- N_2^μ, quadratic in k, whose k-integral diverges both in the UV and in the IR domain: then, it contributes only to $F_1(0)$ and so we have to consider only the constant contribution in order to compute $F_2(0)$.

Also, via a Wick rotation and a shift to polar coordinates, we find that

$$\int \frac{\mathrm{d}^4 k}{(2\pi)^4} \frac{1}{(k^2 - C + i\varepsilon)^3} = \frac{-i}{32\pi^2 C} \,. \qquad (2.14)$$

At this point we substitute (2.14) in the integral expression (2.13), retaining ourselves to the term constant in k. In fact, we will extract $F_2(0)$ from that. Also, we may let $\lambda \to 0$ since the integral with only N_0^μ is no more IR divergent and, with the muons on-shell and $q^2 = 0$, we obtain $C = M^2(y+z)^2$.

Now it is possible to use the projection technique to extract the form factor, but we only quote the results and we refer a more interested reader to (*1*, pp. 173-179).

If one has a matrix element like

$$\Lambda^\mu = \gamma^\mu F_1(q^2) + \frac{i}{2M}\sigma^{\mu\nu}q_\nu F_2(q^2) \,, \qquad (2.15)$$

5 $\frac{1}{ABC} = \Gamma(3)\int_0^1 \mathrm{d}y \int_0^{1-y} \mathrm{d}z \frac{1}{[A+(B-A)y+(C-A)z]^3}$, where Γ is the Euler's function.

the form factors F_i $(i = 1, 2)$ can be extracted as in the following:

$$F_i = Tr\left[P^\mu_{F_i}\Lambda_\mu\right]\big|_{p_i^2=M^2}\,,$$

where

$$P_{F_i} \equiv (\not{p}' + M)\left[c_{1i}\,\gamma^\mu + \frac{c_{2i}}{2M}(p+p')^\mu\right](\not{p} + M)$$

with (for sake of completeness we mention all the coefficients, although only two of them are necessary for our calculation)

$$c_{11} = \frac{1}{2(d-2)(q^2-4M^2)}\,, \qquad c_{12} = \frac{-2M^2}{q^2(d-2)(q^2-4M^2)}\,,$$
$$c_{21} = c_{11}\frac{4M^2(d-1)}{q^2-4M^2}\,, \qquad c_{22} = c_{12}\frac{q^2(d-2)+4M^2}{q^2-4M^2}\,.$$

Then, by claiming that $\overline{u}' N_0^\mu u$ has the same Lorentz structure of $\overline{u}'\Lambda^\mu u$ in (2.15), we obtain:

$$F_2(0) = -\mu^{\frac{3\epsilon}{2}}\frac{4\pi\alpha}{32\pi^2}\,2\int_0^1 \mathrm{d}y\int_0^{1-y}\mathrm{d}z\frac{Tr\left[P^\mu_{F_i}N_{0,\mu}\right]}{M^2(y+z)^2}$$

which, after evaluating the trace and taking the limits $d \to 4$ and $q^2 \to 0$, eventually provides

$$F_2(0) = -\frac{1}{4}\frac{\alpha}{\pi}\int_0^1 \mathrm{d}y\int_0^{1-y}\mathrm{d}z\frac{4M^2(-1+y+z)(y+z)}{M^2(y+z)^2} = \frac{1}{2}\left(\frac{\alpha}{\pi}\right)$$

and this is the already mentioned result for the one-loop QED contribution to a_μ.

2.3.2 *Higher-order QED contribution*

In this section we will briefly discuss higher order contributions from QED diagrams, organizing the following paragraphs according to the number of loops which appear in the relevant diagrams.

Two-Loop

At fourth order in QED there are nine diagrams contributing to a_μ. Among them, six are obtained by attaching two virtual photons to the muon lines and contribute to the universal coefficient. The other three are obtained by inserting in the virtual photon line a vacuum polarization due to lepton loops: respectively, one contributes to $A_1^{(4)}$ (universal), one to $A_2^{(4)}(m_\mu/m_e)$ and one to $A_2^{(4)}(m_\mu/m_\tau)$.

An analytic result for all the coefficients has been known since the early Sixties (24)-(25)-(26), and it was later simplified by the use of dilogarithm properties[6] (5). In fact, knowing that the uncertainty

6 The dilogarithm is defined as $\mathrm{Li}_2(z) \equiv -\int_0^z \mathrm{d}t\,\log(1-t)/t$.

comes from the error on the experimental measure for the lepton masses ratio, one gets (5):

$$\begin{aligned} A_1^{(4)} &= -0.328\,478\,965\,579\ldots \\ A_2^{(4)}(m_\mu/m_e) &= 1.094\,258\,3111\,(84)\ldots \\ A_2^{(4)}(m_\mu/m_\tau) &= 0.000\,078\,064\,(25)\ldots \end{aligned}$$

Adding up the three equations and adding in quadrature the uncertainties of the second and the third (since we assume that the two different mass ratios were measured independently), one obtains the two-loop QED coefficient C_2 as the sum of the three contributions (5):

$$C_2 = 0.765\,857\,410\,(26)$$

If we compute the two-loop contribution to a_μ, $C_2(\alpha/\pi)^2$, we get a tiny uncertainty: $0.01 \cdot 10^{-11}$.

Three-Loop

At sixth order in QED there are more than one hundred diagrams contributing to a_μ. However, there exists an analytic expression of all the coefficients, whose computation ended in the late Nineties.

In particular, the universal coefficient originates from 72 diagrams (27)-(28) and the result reads (5):

$$A_1^{(6)} = 1.181\,241\,4566\ldots$$

On the other hand, the coefficient $A_2^{(6)}(m/M)$, being $m = m_\mu$ and $M = m_e$ or m_τ, comes from 36 diagrams containing electron or tau vacuum polarizations (29) and 12 due to so-called light-by-light scattering diagrams with electron or tau loops (30). As a result (5):

$$\begin{aligned} A_2^{(6)}(m_\mu/m_e) &= 22.868\,380\,02\,(20) \\ A_2^{(6)}(m_\mu/m_\tau) &= 0.000\,360\,51\,(21) \end{aligned}$$

Eventually, at this order there are also diagrams involving both electron and tau loops (31), whose contribution is given by the coefficient (5):

$$A_3^{(6)}(m_\mu/m_e, m_\mu/m_\tau) = 0.000\,527\,66\,(17)\,,$$

where the uncertainty is due to the experimental error on m_μ/m_τ.

Combining the above mentioned three-loop results one obtains the sixth-order QED coefficient C_3 (5):

$$C_3 = 24.050\,509\,64\,(43)\,. \tag{2.16}$$

If we compute the three-loop contribution to a_μ, $C_3(\alpha/\pi)^3$, we get a $O(10^{-14})$ negligible uncertainty. Besides, numerical methods were also developed for the evaluation of the three-loop set of diagrams.

Four-Loop

At eighth order in QED there are more than one thousand diagrams contributing to a_μ. Both a semi-analytical (based on an asymptotic expansion) and a numerical evaluation were accomplished by Steinhauser and collaborators (32) and Kinoshita and collaborators (3), respectively. Also, it has been recently obtained a remarkable result from Laporta (33) for the universal contribution with the astonishing precision of 1100 digits.

The following are the more recent results for each coefficient. From (32) we read:

$$\begin{aligned} A_1^{(8)} &= -1.87\,(12) \\ A_2^{(8)}(m_\mu/m_e) &= 132.86\,(48) \\ A_2^{(8)}(m_\mu/m_\tau) &= 0.042\,4941\,(53) \\ A_3^{(8)}(m_\mu/m_e, m_\mu/m_\tau) &= 0.062\,722\,(10)\,, \end{aligned}$$

from (3):

$$\begin{aligned} A_1^{(8)} &= -1.912\,98\,(84) \\ A_2^{(8)}(m_\mu/m_e) &= 132.6852\,(60) \\ A_2^{(8)}(m_\mu/m_\tau) &= 0.04234\,(12) \\ A_3^{(8)}(m_\mu/m_e, m_\mu/m_\tau) &= 0.06272\,(4) \end{aligned}$$

and eventually from (33):

$$A_1^{(8)} = -1.912\,245\,764\,9264\ldots\,,$$

where the errors are due to the numerical procedure, both in (32) and in (3).

Combining the above mentioned four-loop results, one obtains the four-loop QED contribution to a_μ, $a_\mu^{(8)}$, from (32):

$$a_\mu^{(8)} = (-5.44\,(35) + 386.77\,(1.40) + 0.12371\,(15) + 0.18259\,(29)) \cdot 10^{-11}$$

and from (3):

$$a_\mu^{(8)} = (-5.568\,(2) + 386.264\,(17) + 0.12326\,(35) + 0.18259\,(12)) \cdot 10^{-11}$$

If one computes the final uncertainty in both cases, the result is about two orders of magnitude smaller than the experimental one.

Five-Loop

At tenth order in QED there are more than ten thousand diagrams contributing to a_μ and at present there exists only a numerical evaluation of them. The results by Kinoshita and collaborators read (3):

$$C_5 = 753.29\,(1.04)\,,$$

where the uncertainty is attributed entirely to the statistical fluctuation in the Monte-Carlo integration of Feynman amplitudes.

Summing up the QED results we have quoted, also reported in Table 2.1, we finally obtain

$$a_\mu^{\text{QED}} = 116\,584\,718.951\,(9)\,(19)\,(7)\,(77)\cdot 10^{-11}\,,$$

where the first error is due to the lepton mass ratios, the second and the third to the $O(\alpha^4)$ and $O(\alpha^5)$ terms (the other contributions yield smaller uncertainties), and the fourth to the uncertainty of α, whose best non-QED experimental value is the one obtained from the measurement of h/m_{Rb}, combined with the very precisely known Rydberg constant and m_{Rb}/m_e (34):

$$\alpha^{-1} = 137.035\,999\,049\,(90)\,.$$

All the errors combined yield $\delta a_\mu^{\text{QED}} = 0.08\cdot 10^{-11}$.

Table 2.1: QED contributions to a_μ.

$O(\alpha^n)$	$\times 10^{-11}$
$n=1$	116 140 973.318(77)
$n=2$	413 217.6291(90)
$n=3$	30 141.902 48(41)
$n=4$	381.008(19)
$n=5$	5.0938(70)

2.4 ELECTROWEAK CONTRIBUTION TO a_μ

Differently from the QED contribution, the EW one is in general much more suppressed, and particularly by a factor $(m_\mu/m_W)^2$, where m_W is the mass of the charged boson W.

One-Loop

The one-loop EW contribution is known analytically since 1972 (35), (36),(37), (38), (39):

$$a_\mu^{\text{EW}}(\text{1-loop}) = \frac{5G_F m_\mu^2}{24\sqrt{2}\pi^2}\left[1+\frac{1}{5}(1-4\sin^2\theta_W)^2 + O\Big(\frac{m_\mu^2}{m_{Z,W,H}^2}\Big)\right],$$

where G_F is the Fermi coupling constant, θ_W is the Weinberg angle and $M_{Z,W,H}$ are the W-, Z- and Higgs boson masses, respectively. We may also assert that the Higgs contribution is safely negligible, being of the order of 10^{-14}. This analytic result yields:

$$a_\mu^{\text{EW}}(\text{1-loop}) = (194.82 \pm 0.02)\cdot 10^{-11}\,.$$

Two-loop

On the other hand, while the experimental accuracy was growing year after year, leading to a result with a precision one-third as large as the one-loop contribution, it turned out to be necessary to consider

the two-loop EW contribution too. There came a little surprise, since the latter led to a significant reduction of the one-loop result.

While one could have expected the appearance of terms proportional to $(\alpha/\pi)\, a_\mu^{\rm EW}(1\text{-loop})$, which would have been negligible, and terms enhanced by large logarithms like $\log\left(m_{Z,W}/m_f\right)$ (m_f is a fermion mass scale, much smaller than $m_{Z,W}$), the final result was even larger, enough to reduce the one-loop contribution.

The two-loop contributions are usually split in a fermionic part, including all diagrams which involve closed fermion loops, and a bosonic part, containing all the other diagrams, e.g. hadronic photon-Z mixing and quark triangle loops attached to the muon line via a virtual photon and a Z. The former, computed in the free quark approximation or via a dispersion relation,[7] has a much smaller contribution (*40*) than the latter, also computed in the free quark approximation (*41*).

Nowadays, the result is (*42*):

$$a_\mu^{\rm EW}(2\text{-loop}) \simeq -41.23\,(1)\cdot 10^{-11}\,,$$

where the error is due to the current quark mass uncertainty, unknown three-loop effects (studied in (*43*) via renormalization group analysis) and hadronic loop uncertainties.

Summing up the two quoted results one obtains (*42*):

$$a_\mu^{\rm EW} = (153.6 \pm 1.0)\cdot 10^{-11}\,.$$

2.5 HADRONIC CONTRIBUTION TO a_μ

In this section we are dealing with the hadronic contribution to the muon anomalous magnetic moment, which originates from QED diagrams involving hadrons.[8]

Particularly, the most sizable hadronic effect is the $O(\alpha^2)$ hadronic vacuum polarization (HVP) insertion in the internal photon line of the leading one-loop muon vertex diagram. This will be treated in some details in section 2.5.1, representing both the main uncertainty in the SM theoretical prediction of a_μ and the motivation for calculating the muon-electron elastic scattering cross section at NLO.

Moreover, at order $O(\alpha^3)$ we have other diagrams contributing with a smaller result, but still of relevance if one takes into account the accuracy which future a_μ measurement will reach. These contributions are much more concisely treated in section 2.5.2.

7 See 2.5.1.

8 One should note that the two-loop EW diagrams involving hadrons have been already mentioned in the previous section.

2.5.1 *Leading-order hadronic contribution*

Since it involves low-energy QCD, which cannot be treated perturbatively, the evaluation of the diagram where a hadronic blob shows up, has to be fulfilled by using different methods. In particular, it has been demonstrated in the Sixties, by Bouchiat and Michel (44), that the result may be obtained with the help of an analyticity- and unitarity-based approach.

Analiticity

Let us first consider a complex function of the Mandelstam variable s, $f(s)$, which has a branch cut along the real positive axis in the s-plane, starting at $s = s_0$ and extending to infinity, and which is real below s_0. Then, we may write $f(s)$ in terms of a Cauchy integral representation

$$f(s) = \frac{1}{2\pi i} \oint_{\mathcal{C}} \frac{ds' f(s')}{s' - s}, \tag{2.17}$$

where $\mathcal{C}$ is the contour shown in Figure 2.1.

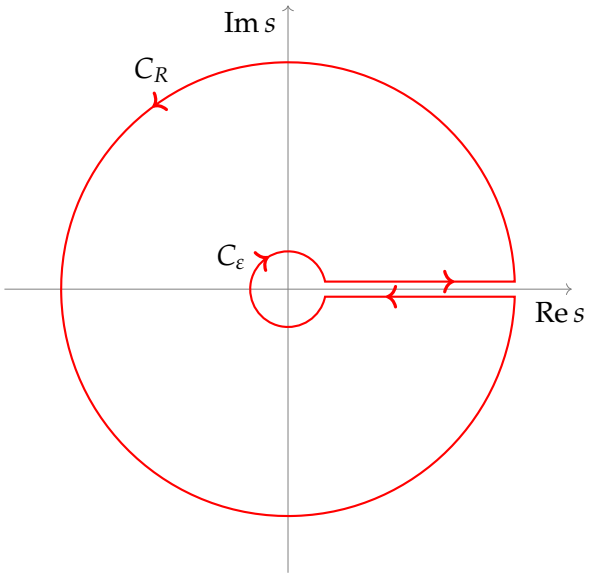

Figure 2.1: In red, the contour $\mathcal{C}$. The centre of the circles is at $s = s_0 + i0$.

Now, assuming that $f(s)$ may be defined for complex s in the upper half s-plane, the Schwartz reflection principle allows us to extend the domain of $f(s)$ to the lower half s-plane by $f(s^*) = f^*(s)$, where * represents the complex conjugation.

Then, as a contribution from the branch cut (real $s > s_0$) we have:

$$\lim_{\varepsilon \to 0^+} f(s + i\varepsilon) - f(s - i\varepsilon) = 2i \operatorname{Im} f(s)$$

by which we may rewrite (2.17), for any s inside $\mathcal{C}$, as

$$f(s) = \frac{1}{2\pi i} \int_{s_0}^{\infty} \frac{ds' \, 2i \operatorname{Im} f(s')}{s' - s} + \frac{1}{2\pi i} \int_{\mathcal{C}_R + \mathcal{C}_\varepsilon} \frac{ds' f(s')}{s' - s}.$$

If the contributions from $\mathcal{C}_R$ and $\mathcal{C}_\varepsilon$ vanish in the limits $\varepsilon \to 0$ and $R \to \infty$, namely $f(s)$ falls off sufficiently rapidly in those limits, the latter equation yields a *dispersion relation* (DR) for $f(s)$:

$$f(s) = \frac{1}{\pi} \int_{s_0}^{\infty} \frac{\mathrm{d}s' \, \mathrm{Im}\, f(s')}{s' - s} \,. \tag{2.18}$$

If the contribution from the circle $\mathcal{C}_R$ does not vanish, we may subtract $f(b)$ from $f(s)$, for any b in the domain of $f(s)$, and let the integrand vanish faster at infinity via a factor $\propto 1/s'$:

$$f(s) - f(b) = \frac{s-b}{2\pi \mathrm{i}} \int_{s_0}^{\infty} \frac{\mathrm{d}s' \, 2\mathrm{i}\, \mathrm{Im}\, f(s')}{(s'-s)(s'-b)} + \frac{s-b}{2\pi \mathrm{i}} \int_{\mathcal{C}_R + \mathcal{C}_\varepsilon} \frac{\mathrm{d}s' \, f(s')}{(s'-s)(s'-b)}$$

which reduces to

$$f(s) - f(b) = \frac{s-b}{\pi} \int_{s_0}^{\infty} \frac{\mathrm{d}s' \, \mathrm{Im}\, f(s')}{(s'-s)(s'-b)} \tag{2.19}$$

if now the circle contribution vanishes. This latter equation is defined as a *subtracted dispersion relation* (SDR) for $f(s)$.

Since we have to consider the LO HVP insertion in the internal photon line of the leading one-loop muon vertex diagram, we try to apply the just recalled properties of analytic functions to the HVP function, whose analyticity is granted by causality.

Let us define the HVP function as $\Pi'_{\mathrm{had}}(q^2)$, where q is the 4-momentum associated to the internal photon line. Moreover, we know that $\Pi'_{\mathrm{had}}(q^2)$ exhibits a UV singularity, so that we shall consider a SDR with $b = 0$ and we may write from (2.19):

$$\Pi'_{\mathrm{had}}(q^2) - \Pi'_{\mathrm{had}}(0) = \frac{q^2}{\pi} \int_{4m_\pi^2}^{\infty} \frac{\mathrm{d}s \, \mathrm{Im}\, \Pi'_{\mathrm{had}}(s)}{s(s - q^2)} \tag{2.20}$$

In fact, we know that $\Pi'_{\mathrm{had}}(q^2 = 0)$ corresponds to the counter-term which renormalizes $\Pi'_{\mathrm{had}}(q^2)$; henceforth we define for brevity

$$\overline{\Pi}'_{\mathrm{had}}(q^2) \equiv \Pi'_{\mathrm{had}}(q^2) - \Pi'_{\mathrm{had}}(0)$$

i.e. the renormalized HVP function. Also, we remark that m_π is the pion mass and $4m_\pi^2$ corresponds to the hadron production threshold, namely the q^2 value at which the branch cut for $\Pi'_{\mathrm{had}}(q^2)$ starts.

Unitarity

If (2.20) establishes what we may infer from the analyticity of the HVP function, unitarity considerations may offer a useful tool to express $\mathrm{Im}\, \Pi'_{\mathrm{had}}(s)$ in terms of experimentally measured cross sections.

In particular, unitarity implies the *optical theorem*, which states, in a scattering process framework, that the imaginary part of the forward scattering amplitude of an elastic process

$$a + b \to a + b$$

is proportional to the sum over all possible final states

$$a + b \to \text{'anything'}\,.$$

In the HVP case, which is crucial for our discussion, one may find that this yields:

$$\operatorname{Im}\Pi'_{\text{had}}(s) = \frac{s}{4\pi\alpha}\,\sigma_{\text{tot}}(e^+e^- \to \text{hadrons})\,.$$

This latter equation may be also reformulated as

$$\operatorname{Im}\Pi'_{\text{had}}(s) = \frac{\alpha}{3}\,R_{\text{had}}(s)\,, \tag{2.21}$$

where

$$R_{\text{had}}(s) = \sigma_{\text{tot}} \Big/ \frac{4\pi\alpha^2}{3s}$$

is the ratio between the hadronic inclusive cross section σ_{tot}, which is known from the experiments as it cannot be perturbatively calculated, and the $e^+e^- \to \mu^+\mu^-$ tree level cross section, computed in the relativistic limit $s \gg 4m_\mu^2$, which is used as a normalization factor.

Now, by combining (2.20) and (2.21), we eventually obtain:

$$\overline{\Pi}'_{\text{had}}(q^2) = \frac{\alpha q^2}{3\pi}\int_{4m_\pi^2}^{\infty}\frac{\mathrm{d}s\,R_{\text{had}}(s)}{s(s-q^2)}\,. \tag{2.22}$$

This is a crucial result in order to compute the LO hadronic contribution to a_μ, since it bypasses the issue of calculating the low energy QCD contribution to it. Then, we apply it right away to the calculation of our interest.

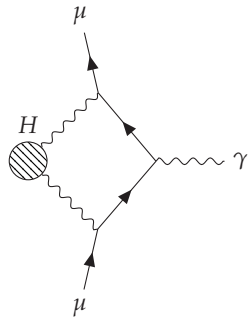

Since we aim to compute the contribution to a_μ from the diagram aside, where a hadronic blob H was inserted in the virtual photon line, we shall recall some features about the photon propagator, following Jegerlehner's book (1).

Working in the Feynman gauge $\xi = 1$, like we did and will do throughout the whole thesis, the free photon propagator has the form

$$\mathrm{i}D^{\mu\nu}(q^2) = \frac{-\mathrm{i}g^{\mu\nu}}{q^2 + i\varepsilon}\,,$$

where the virtual photon carries a 4-momentum q. If we consider the so called Dyson series of self energy insertions, then it becomes, omitting the metric tensor $g^{\mu\nu}$, which acts equally on every term, and the $i\varepsilon$ prescription,

$$\begin{aligned}\mathrm{i}D'(q^2) &= \frac{-\mathrm{i}}{q^2} + \frac{-\mathrm{i}}{q^2}(-\mathrm{i}\Pi)\frac{-\mathrm{i}}{q^2} + \frac{-\mathrm{i}}{q^2}(-\mathrm{i}\Pi)\frac{-\mathrm{i}}{q^2}(-\mathrm{i}\Pi)\frac{-\mathrm{i}}{q^2} + \ldots \\ &= \frac{-\mathrm{i}}{q^2}\left[1 + \left(\frac{-\Pi}{q^2}\right) + \left(\frac{-\Pi}{q^2}\right)^2 + \ldots\right] \\ &= \frac{-\mathrm{i}}{q^2}\left[\frac{1}{1-\Pi/q^2}\right] = \frac{-\mathrm{i}}{q^2 - \Pi(q^2)}\,.\end{aligned}$$

Further, by gauge invariance, we know that the photon must remain massless after including radiative corrections, which affects $\Pi(q^2)$. This requires that $\Pi(q^2) = \Pi(0) + q^2\Pi'(q^2)$, with $\Pi(0) = 0$ following from the transversality condition. Then, as a final result, we obtain the dressed photon propagator

$$iD'^{\mu\nu}(q^2) = \frac{-ig^{\mu\nu}}{q^2[1-\Pi'(q^2)]} + \text{gauge terms} \tag{2.23}$$

which is what we really need to study the hadronic bubble.

In fact, the physically relevant $g^{\mu\nu}$ term of the full photon propagator may also be written as

$$\frac{-ig^{\mu\nu}}{q^2[1-\Pi'(q^2)]} \simeq \frac{-ig^{\mu\nu}}{q^2}\Big(1+\Pi'(q^2)-(\Pi'(q^2))^2+\dots\Big).$$

Therefore, one may note that the hadronic bubble H insertion in the photon propagator leads to the following straightforward substitution for a photon virtual line:

$$\frac{-ig^{\mu\nu}}{q^2} \to \frac{-ig^{\mu\nu}[\Pi'_H(q^2)-\Pi'_H(0)]}{q^2}, \tag{2.24}$$

where we have already subtracted the counter-term $\Pi'_H(0)$ from $\Pi'_H(q^2)$ in order to cancel the UV divergence of the latter. For brevity we also define the renormalized photon self energy $\overline{\Pi}'_H \equiv \Pi'_H(q^2) - \Pi'_H(0)$.

At this stage, by using (2.22), we easily find that the NLO contribution from (2.24) becomes

$$\frac{-\overline{\Pi}'_H(q^2)}{q^2} = \frac{\alpha}{3\pi}\int_{4m_\pi^2}^{\infty}\frac{ds\,R_H(s)}{s(s-q^2)}. \tag{2.25}$$

We also note that the only q dependence under the last integral shows up in the denominator as $-(q^2-s)$. Then, it is possible to write the LO hadronic contribution to a_μ by substituting

$$\frac{-ig^{\mu\nu}}{q^2} \to \frac{-ig^{\mu\nu}}{q^2-s}$$

in the lower order expression, namely (2.12), with $\lambda = 0$.

Following a similar path but introducing three Feynman parameters which let the expression assume a slightly clearer shape,[9] one obtains

$$F_2^H(q^2) = \frac{\alpha^2}{3\pi^2}\int_0^1 dxdydz\int_{4m_\pi^2}^{\infty}\frac{ds}{s}\frac{\delta(x+y+z-1)\,R_H(s)(1-z)zM^2}{(1-z)^2M^2-xyq^2+sz}$$

which yields

$$a_\mu^{\text{HLO}} = F_2^H(q^2=0) = \frac{\alpha}{\pi}\int_{4m_\pi^2}^{\infty}\frac{ds}{s}\,\text{Im}\,\Pi'_H(s)K(s) \tag{2.26}$$

9 $\frac{1}{ABC} = \Gamma[3]\int_0^1 dx\int_0^1 dy\int_0^1 dz\frac{\delta(x+y+z-1)}{(Ax+By+Cz)^3}$

or

$$a_\mu^{\mathrm{HLO}} = F_2^H(q^2=0) = \frac{\alpha^2}{3\pi^2}\int_{4m_\pi^2}^{\infty}\frac{\mathrm{d}s}{s}\,R_H(s)K(s)\,, \tag{2.27}$$

where

$$K(s) = \int_0^1 \frac{x^2(1-x)}{x^2+(s/M^2)(1-x)}\,. \tag{2.28}$$

Time-like approach

Hence (2.27) offers an approach to overcome long-distance QCD issues appearing in the LO hadronic contribution to a_μ calculation. Since it makes use of hadronic e^+e^- annihilation data, thus involving a positive squared momentum transfer, we will call it *time-like approach*.

Detailed evaluations of the dispersive integral in (2.27) have been carried out by several authors, being this contribution of the order $7000\cdot 10^{-11}$, very large compared with the current experimental uncertainty $\delta a_\mu^{\mathrm{exp}} = 60\cdot 10^{-11}$. Here we only present the most recent results from (*45*), (*46*) and (*47*), respectively:

$$\begin{aligned} a_\mu^{\mathrm{HLO}} &= 6949\,(37.2)\,(21)\cdot 10^{-11} \\ a_\mu^{\mathrm{HLO}} &= 6909.6\,(4.65)\cdot 10^{-11} \\ a_\mu^{\mathrm{HLO}} &= 6923\,(4.2)\cdot 10^{-11}\,, \end{aligned}$$

where the first (or unique) error is due to the experimental measurement of hadronic e^+e^- annihilation, while the second to final state radiation effects.

Space-like approach

As one may note, this approach bypasses QCD long-distance problems, but suffers from the experimental uncertainty by which we measure the hadronic e^+e^- annihilation. In September 2016 a new experiment, MUonE, has been proposed (*10*). It aims to measure the running of α in the space-like region by scattering 150 GeV muons on atomic electrons of low-Z target through the elastic process $\mu\,e\to\mu\,e$. As we will show, the differential cross section of that process, measured as a function of the squared 4-momentum transfer $t<0$, provides direct sensitivity to the LO hadronic contribution to a_μ.

In (*9*) it was noticed that, exchanging the integrations and evaluating the subtracted dispersion relation in (2.26), one gets:

$$\begin{aligned} a_\mu^{\mathrm{HLO}} &= \alpha\int_0^1 \mathrm{d}x(1-x)\int_{4m_\pi^2}^{\infty}\frac{\mathrm{d}s}{\pi s}\,\mathrm{Im}\,\Pi'_H(s)\,\frac{x^2}{x^2+(s/M^2)(1-x)} \\ &= \frac{\alpha}{\pi}\int_0^1 \mathrm{d}x(1-x)\frac{-1}{1+\Pi'_H(t)} \\ &= \frac{\alpha}{\pi}\int_0^1 \mathrm{d}x(1-x)\Delta\alpha_H[t(x)]\,, \end{aligned} \tag{2.29}$$

where $\Delta\alpha_H(t)$ is the hadronic contribution to the running of α, evaluated at

$$t(x) = \frac{x^2M^2}{x-1} < 0 \tag{2.30}$$

the space-like squared 4-momentum transfer. The second equality is obtained by observing that, with t defined as in (2.30),

$$\frac{x^2}{x^2 + (s/M^2)(1-x)} = -t\frac{1}{s-t}\,.$$

On the other hand, the last equality is obtained by recalling that the shape of the dressed photon propagator, see (2.23), implies that the charge has to be replaced by a running charge:

$$e^2 \to e^2(t) = \frac{e^2(0)Z_3}{1+\Pi'(t)}\,,$$

where Z_3 is the renormalization factor fixed by the condition that at $t \to 0$ one obtains the charge in the Thomson limit. Thus, the renormalized charge is

$$e^2 \to e^2(t) = \frac{e^2(0)}{1+[\Pi'(t)-\Pi'(0)]}\,,$$

which yields, in terms of the fine structure constant,

$$\alpha(t) = \frac{\alpha(0)}{1-\Delta\alpha(t)}\,,$$

where $\Delta\alpha(t) = -[\Pi'(t)-\Pi'(0)]$. At this stage, it is easy to obtain (2.29) via the substitution $\Pi' \to \Pi'_H$, since we are interested in the hadronic case. We would also like the reader to notice that, in contrast with the integrand function of (2.27), the integrand in (2.29) is smooth and free of resonances.

The above discussion explains why it has been decided to compute the muon−electron elastic scattering cross section. In fact, the hadronic contribution $\Delta\alpha_H(t)$ can be extracted by subtracting from $\Delta\alpha(t)$ the purely leptonic part, which may be calculated order by order in perturbation theory. Finally, we point out that the aimed experiment accuracy is 10 ppm; then, we will take account of this number while computing the NLO muon−electron cross section, in order to neglect smaller contributions.

2.5.2 *Higher-order hadronic contribution*

We close the section dedicated to the muon $g-2$, by briefly giving an account of the hadronic higher order (HHO) contributions. Usually, they are split in diagrams with vacuum polarization insertions (vap), whose result may be expressed in terms of experimental observables, or light-by-light scattering (lbl), whose result relies at present on purely theoretical considerations.

The latest results read from (*45*) and (*48*) respectively:

$$a_\mu^{\mathrm{HHO}}(\mathrm{vap}) = -98.4\,(0.6)\,(0.4)\cdot 10^{-11}$$
$$a_\mu^{\mathrm{HHO}}(\mathrm{lbl}) = 116\,(40)\cdot 10^{-11}\,,$$

where the (vap) contribution first error is due to the experimental measure of hadronic e^+e^- annihilation, while the second to final state radiation effects; the (lbl) error covers almost all values obtained in other different publications.

2.6 THEORETICAL PREDICTION VS MEASUREMENT

In the following we sum up all the results of this chapter, adding the latest measurement of a_μ by the experiment E821 at Brookhaven (*49*), (*50*). As we have already mentioned, more precise measurements will be obtained in the next few years by Fermilab and J-PARC, hopefully with an accuracy of 0.14 ppm.

$$\begin{aligned} a_\mu^{\mathrm{SM}} &= a_\mu^{\mathrm{QED}} + a_\mu^{\mathrm{EW}} + a_\mu^{\mathrm{HLO}} + a_\mu^{\mathrm{HHO}}(\mathrm{vap}) + a_\mu^{\mathrm{HHO}}(\mathrm{lbl}) \\ &= 116\,591\,840\,(59)\cdot 10^{-11}\,, \end{aligned}$$

$$a_\mu^{\mathrm{exp}} = 116\,592\,089\,(63)\cdot 10^{-11}.$$

Hence the long-standing 3-4 standard deviation discrepancy between the theoretical prediction and the experimental value:

$$a_\mu^{\mathrm{exp}} - a_\mu^{\mathrm{SM}} = 249\,(87)\cdot 10^{-11}\,.$$

3

MUON−ELECTRON ELASTIC SCATTERING

In this chapter the SM calculation for the muon−electron elastic scattering cross section at NLO is presented.

The kinematics in the laboratory frame of reference is recalled in section 3.1, the LO contribution is computed in section 3.2, the one-loop virtual contribution is considered in section 3.3, soft photon emission is taken into account via Bremsstrahlung diagrams at LO in section 3.4. Finally, the result is presented in section 3.5, also referring the reader to the appendix B for the explicit formulae.

The NLO QED corrections to this cross section were computed long time ago in (51), (52), (53), (54), (55) and (56), and revisited more recently in (57). As a first check, we recalculated these corrections and found perfect agreement with (57), although unsolved integrals still show up in the final expressions of that reference. We also note that some of the pioneering publications, like (52) and (54), contain typos or errors, so that they cannot be directly employed. Then, aim of this work is to obtain a correct and usable result, which may be directly tested by experiments like MUonE.

3.1 KINEMATICS IN THE LAB FRAME

The process is represented as a standard $2 \to 2$ elastic scattering of muons (μ^-) on electrons (e^-), whose masses are defined M and m, respectively. We will not make any massless approximation, keeping both M and m along the calculation, and in the various diagrams the electron lines will be thin and black, while the muon lines red and thick.

Further, the following conventions and notations are used: q_1 and q_2 are the incoming and outgoing muon 4-momenta; p_1 and p_2 are the incoming and outgoing electron 4-momenta; metric and Dirac matrices identities are recalled in app. A; s, t and u are the Mandelstam invariants defined by

$$\begin{aligned} s &= (p_1 + q_1)^2 = (p_2 + q_2)^2 \\ t &= (p_1 - p_2)^2 = (q_1 - q_2)^2 \\ u &= (p_1 - q_2)^2 = (p_2 - q_1)^2 \\ s + t + u &= 2M^2 + 2m^2 \end{aligned} \tag{3.1}$$

In the lab frame, in a fixed-target experiment, we shall have:

$$p_1 = \begin{pmatrix} m \\ \mathbf{0} \end{pmatrix} \quad q_1 = \begin{pmatrix} E_{1\mu} \\ \mathbf{q_1} \end{pmatrix} \quad p_2 = \begin{pmatrix} E_{2e} \\ \mathbf{p_2} \end{pmatrix} \quad q_2 = \begin{pmatrix} E_{2\mu} \\ \mathbf{q_2} \end{pmatrix}$$

Once we defined all these quantities, we may compute the Lorentz-invariant phase space factor for a two-body final state, $\mathrm{d}\Pi_2$. In fact, the differential cross section $\mathrm{d}\sigma$ of our interest will have the following shape:

$$\mathrm{d}\sigma = (2\pi)^4 \delta^{(4)}(q_2 + p_2 - q_1 - p_1) \frac{\mathcal{X}}{2\Lambda^{1/2}(s, m^2, M^2)} \mathrm{d}\Pi_2 \,, \tag{3.2}$$

where $\mathcal{X}$ is the renormalized and unpolarized $\mathcal{T}$-matrix element, Λ is the Källén function, defined by $\Lambda(x, y, z) = x^2 + y^2 + z^2 - 2xy - 2yz - 2zx$, and

$$\mathrm{d}\Pi_2 = \frac{\mathrm{d}^3\mathbf{p_2}}{(2\pi)^3 2E_{2e}} \frac{\mathrm{d}^3\mathbf{q_2}}{(2\pi)^3 2E_{2\mu}} \,.$$

We integrate the 4-momentum conservation delta over the outgoing muon 3-momentum ($\mathbf{q_2}$), then we shift to spherical polar coordinates by writing

$$\mathrm{d}^3\mathbf{p_2} = |\mathbf{p_2}|^2 \mathrm{d}|\mathbf{p_2}| \mathrm{d}\cos\theta \mathrm{d}\varphi \,,$$

where $\theta \in (0, \pi)$ is the angle between the incoming muon and the outgoing electron, $\varphi \in (0, 2\pi)$, and eventually we find, from (3.2),

$$\mathrm{d}\sigma = \frac{\mathcal{X}\, \delta(E_{1\mu} + m - E_{2\mu} - E_{2e})}{32\pi^2 \Lambda^{1/2}(s, m^2, M^2)} \frac{|\mathbf{p_2}|}{E_{2\mu} E_{2e}} E_{2e}\, \mathrm{d}E_{2e}\, \mathrm{d}\cos\theta\, \mathrm{d}\varphi \,, \tag{3.3}$$

where we used $E_{2e}\, \mathrm{d}E_{2e} = |\mathbf{p_2}|\, \mathrm{d}|\mathbf{p_2}|$, which follows by differentiation from $m^2 = E_{2e}^2 - |\mathbf{p_2}|^2$.

In order to perform the last delta integration we recall how to write in general $\delta(f(x))$,[1] that is in our case:

$$\delta(E_{1\mu} + m - E_{2\mu} - E_{2e}) = \delta(c - c_0) \left| \frac{\partial(E_{1\mu} + m - E_{2\mu}(E_{2e}, c) - E_{2e})}{\partial c} \right|^{-1}_{c=c_0} \,,$$

where $c \equiv \cos\theta$, c_0 is such that $E_{2\mu}(c_0) = E_{1\mu} + m - E_{2e}$ and $E_{2\mu} = E_{2\mu}(E_{2e}, c)$ by squaring the 3-momentum conservation relation, i.e.

$$\mathbf{q_2} = \mathbf{q_1} - \mathbf{p_2} \quad \leftrightarrow \quad E_{2\mu} = (E_{1\mu}^2 + E_{2e}^2 - m^2 - 2c|\mathbf{q_1}||\mathbf{p_2}|)^{1/2}$$

As a result, by recalling that in the lab frame

$$|\mathbf{q_1}| = \frac{1}{2m} \Lambda^{1/2}(s, m^2, M^2)$$

1 $\delta(f(x)) = \sum_i \delta(x - \bar{x}_i) \left| \frac{\partial f(x)}{\partial x} \right|^{-1}_{x=\bar{x}_i}$, where the equality holds in a distributional sense and $\bar{x}_i$ are the roots of $f(x)$ belonging to the integration domain.

and, from the definition of t in (3.1),

$$\mathrm{d}t = -\frac{\mathrm{d}E_{2e}}{2m}$$

we finally obtain from (3.3), also integrating over φ,

$$\begin{aligned}\mathrm{d}\sigma &= \frac{\delta(c-c_0)E_{2\mu}}{|\mathbf{q_1}||\mathbf{p_2}|}\frac{\mathcal{X}}{16\pi\Lambda^{1/2}(s,m^2,M^2)}\frac{|\mathbf{p_2}|}{E_{2\mu}}\,\mathrm{d}E_{2e}\,\mathrm{d}c \\ &= -\frac{\mathcal{X}}{16\pi\Lambda(s,m^2,M^2)}\,\mathrm{d}t\,.\end{aligned} \tag{3.4}$$

Once the kinematics is set, we may turn to the computation of $\mathcal{X}$, starting from the LO contribution.

3.2 LO CONTRIBUTION

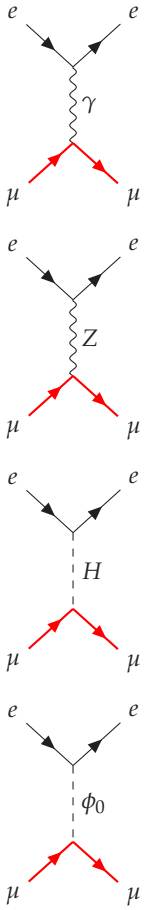

At leading order in the $\xi = 1$ gauge there are four Feynman diagrams contributing to the cross section of the process, which is characterized by neutral currents. They are shown aside and differ in the propagator, being the first a photon, the second a Z-boson, the third a Higgs boson and the fourth a neutral Goldstone boson.

As a consequence, by calling $\mathcal{M}_A$, $\mathcal{M}_Z$, $\mathcal{M}_H$ and $\mathcal{M}_\phi$ the Feynman matrix elements originating from the diagrams with a photon, Z-boson, Higgs boson and Goldstone boson propagator, the LO unpolarized amplitude $\mathcal{X}^{\mathrm{LO}}$ may be written as

$$\begin{aligned}\mathcal{X}^{\mathrm{LO}} &= \frac{1}{4}\sum_{\text{spins}}|\mathcal{M}_A+\mathcal{M}_Z+\mathcal{M}_H+\mathcal{M}_\phi|^2 \\ &= \mathcal{X}_A+\mathcal{X}_Z+\mathcal{X}_H+\mathcal{X}_\phi+\sum_{\substack{I,J=\{A,Z,H,\phi\}\\ I\neq J}}\mathrm{Re}\,\mathcal{X}_{I-J}\,,\end{aligned} \tag{3.5}$$

where the $1/4$ factor shows up since we are averaging over the initial spins of two leptons. It is also clear that the first four terms in the last equality correspond to the squared matrix elements, while the last six ($\mathcal{X}_{I-J} = \mathcal{X}_{J-I}$) originate from the interference between them.

As we described in chapter 1, we are interested in this very process since it might help to obtain a more accurate theoretical prediction to the LO hadronic contribution to a_μ. Besides, one might also foresee that, even though we aim to a very precise result which requires a $\mu - e$ scattering cross section at $O(\alpha^4)$, the contributions from the diagrams involving Higgs-fermion, Z-fermion or Goldstone-fermion couplings are too small to be taken into account.

In particular, the former is the most suppressed contribution, since it is proportional to (mM/v^2), where $v = 246$ GeV is the electroweak vacuum expectation value. The second is also suppressed but, as we will see, the interference term $\mathcal{X}_{A-Z}$ of the Z-boson with the photon

yields a border-line contribution in terms of needed accuracy. The latter is equally suppressed and, in particular, the interference term $\mathcal{X}_{A-\phi}$ is identically zero.

In the following subsections, 3.2.1, 3.2.2 and 3.2.3 respectively, we shall then concentrate on $\mathcal{X}_A$, $\mathcal{X}_{A-Z}$ and $\mathcal{X}_{A-\phi}$. In fact

$$\mathcal{X}^{\mathrm{LO}} = \mathcal{X}_A + 2\,\mathrm{Re}\,\mathcal{X}_{A-Z} + O(\alpha^2)$$

and we would also like to show that $\mathcal{X}_{A-\phi} = 0$.

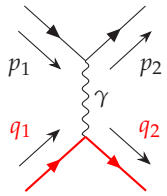

3.2.1 *Photon contribution*

The unpolarized Feynman amplitude originating from the first diagram only is easily computable via the Feynman rules quoted in app. A, yielding

$$\begin{aligned}\mathcal{X}_A &= \frac{1}{4}\sum_{\text{spins}} \frac{e^4}{t^2}\overline{u}(q_1)\gamma^\mu u(q_2)\overline{u}(p_1)\gamma_\mu u(p_2)\overline{u}(p_2)\gamma_\nu u(p_1)\overline{u}(q_2)\gamma^\nu u(q_1)\\ &= \frac{e^4}{4t^2}\,\mathrm{Tr}[\gamma^\mu(\not{q}_1 + M)\gamma^\nu(\not{q}_2 + M)]\;\mathrm{Tr}\big[\gamma_\mu(\not{p}_1 + m)\gamma_\nu(\not{p}_2 + m)\big]\,,\end{aligned}$$

where the trace may be computed using the Dirac matrices identities quoted in app. A. Further, by evaluating in the lab frame the scalar products originating from the trace we obtain

$$\mathcal{X}_A = \frac{2(4\pi\alpha)^2}{t^2} f(s,t)\,, \tag{3.6}$$

where

$$\begin{aligned} f(s,t) &= 2(M^2 + m^2 - s)^2 + 2st + t^2\\ &= 2(M^2 + m^2)^2 - 2su + t^2\end{aligned} \tag{3.7}$$

and the last equality directly follows from 3.1.

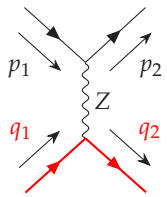

3.2.2 *Photon−Z interference contribution*

The unpolarized Feynman amplitude originating from the first and second diagram interference is also easily computable via the Feynman rules quoted in app. A. As we sketched in section 2.5.1, for the experimental measurement of our interest $s \simeq 0.16\ \mathrm{GeV}^2$ and $t \in (-0.14, 0)\ \mathrm{GeV}^2$. In this low energy regime, namely $|t| \ll M_Z^2$ where M_Z is Z-boson mass, we find

$$\begin{aligned}2\,\mathrm{Re}\,\mathcal{X}_{A-Z} &\simeq \frac{1}{4}\sum_{\text{spins}} 2\,\mathrm{Re}\Big[\frac{-ie^2}{t}\overline{u}(q_1)\gamma^\mu u(q_2)\overline{u}(p_1)\gamma_\mu u(p_2)\frac{ig^2}{\cos^2\theta_W}\times\\ &\times\,\overline{u}(p_2)\gamma_\nu(g_V - g_A\gamma^5)u(p_1)\Big(-\frac{1}{M_Z^2}\Big)\overline{u}(q_2)\gamma^\nu(g_V - g_A\gamma^5)u(q_1)\Big]\\ &= -\frac{4G_F e^2}{\sqrt{2}t}\,\mathrm{Tr}[\gamma^\mu(\not{q}_1 + M)V^\nu(\not{q}_2 + M)]\;\mathrm{Tr}\big[\gamma_\mu(\not{p}_1 + m)V_\nu(\not{p}_2 + m)\big]\,,\end{aligned}$$

where the Z-boson propagator reduces to $-1/M_Z^2$ in the low energy limit, G_F is the Fermi constant, related to the charged vector boson mass M_W or M_Z and $\cos\theta_W$ by

$$\frac{8G_F}{\sqrt{2}} = \frac{g^2}{M_W^2} = \frac{g^2}{M_Z^2\cos^2\theta_W}\,, \tag{3.8}$$

V^μ is a short notation for $\gamma^\mu(g_V - g_A\gamma^5)$, where g_V and g_A are the vectorial and axial couplings, defined via the weak isospin third-component eigenvalue T^3 and the lepton charge Q:

$$g_V = \frac{1}{4}(2T^3 - 4Q\sin^2\theta_W)\,, \qquad g_A = \frac{1}{4}2T^3\,.$$

After computing the trace by the customary Dirac matrices identities and evaluating the scalar products originating from the trace, we eventually obtain for a $\mu^- e^-$ scattering

$$\begin{aligned} 2\mathcal{X}_{A-Z} &= -\frac{64}{\sqrt{2}}\frac{G_F e^2}{t}\left[g_V^2\left((M^2+m^2-s)^2 + st + \frac{t^2}{2}\right) - g_A^2(s-u)\frac{t}{2}\right] \\ &= -4\sqrt{2}\pi\frac{\alpha G_F}{t}\left[f(s,t)(4\sin^2\theta_W - 1)^2 - t(s-u)\right], \end{aligned} \tag{3.9}$$

where we used $T^3 = -1/2$ and $Q = -1$ for charged leptons.

By adding together the results in (3.4), (3.6) and (3.9), we may write

$$\left(\frac{\mathrm{d}\sigma}{\mathrm{d}t}\right)^{\mathrm{LO}} = \left(\frac{\mathrm{d}\sigma}{\mathrm{d}t}\right)_0^{\mathrm{LO}}\Big[1 + \delta_Z(s,t)\Big] + O(\alpha^2)\,, \tag{3.10}$$

where

$$\left(\frac{\mathrm{d}\sigma}{\mathrm{d}t}\right)_0^{\mathrm{LO}} = -\frac{2\pi\alpha^2}{\Lambda(s,m^2,M^2)t^2}\,f(s,t)\,, \tag{3.11}$$

$f(s,t)$ is defined in (3.7) and

$$\delta_Z(s,t) = -\frac{G_F t}{4\sqrt{2}\pi\alpha}\left((4\sin^2\theta_W - 1)^2 - \frac{t(s-u)}{f(s,t)}\right) \tag{3.12}$$

is the correction to the QED contribution to the scattering differential cross section computed at LO.

At this stage one may also wonder how much $\delta_Z(s,t)$ affects the theoretical prediction accuracy, which will be then compared with the experimental one. For the data-taking, a muon beam of 150 GeV will be used on a fixed electron target (*10*). Then it turns out that $s \simeq 0.16$ GeV^2 and $t \in (-0.14, 0)$ GeV^2, i.e. $t \in (-\Lambda(s,m^2,M^2)/s, 0)$ GeV^2. The maximum t-value, i.e. $t = 0$ GeV^2, is reached when $E_{2e} = m$, while the minimum is reached when $E_{2e} \simeq 139.8$ GeV^2. In fact, by energy conservation, E_{2e} is a function of $\cos\theta$:

$$E_{2e} = E_{1\mu} + m - (E_{1\mu}^2 + E_{2e}^2 - m^2 - 2|\mathbf{q_1}|(E_{2e}^2 - m^2)^{1/2}\cos\theta)^{1/2}$$

and the value for E_{2e} which minimizes the last equation, evaluated at $\theta = 0$, is $E_{2e} \simeq 139.8\ \text{GeV}^2$.

Once these facts are known, it is easy to conclude that the maximum value of $\delta_Z(s,t)$ is

$$\delta_Z(s \simeq 0.16, t \simeq -0.14) \simeq 1.5 \cdot 10^{-5}\,,$$

as it is shown in Figure 3.1. This also explains why we did not consider other LO terms contributing to the cross section, in particular the bigger of them, that is $\mathcal{X}_Z$. It is a matter of fact, that this latter contributes proportionally to G_F^2, which offers a contribution much smaller than the maximum value of $\delta_Z(s,t)$.

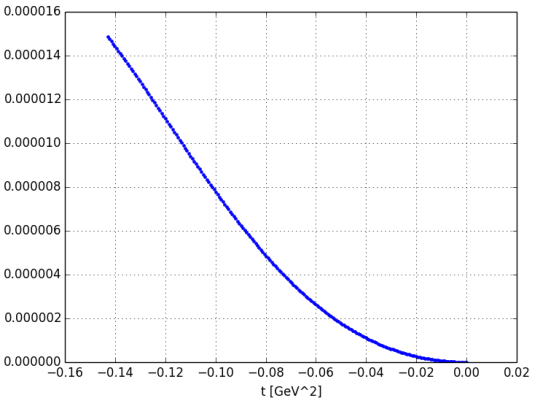

Figure 3.1: On the y-axis, $\delta_Z(s,t)$ as a function of t.

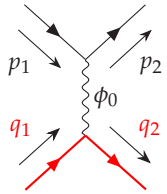

3.2.3 *Photon−Goldstone interference contribution*

The unpolarized Feynman amplitude originating from the first and fourth diagram interference is also easily computable via the Feynman rules quoted in Appendix A. Even in this case we recall that for the experimental measurement of our interest $s \simeq 0.16\ \text{GeV}^2$ and $t \in (-0.14, 0)\ \text{GeV}^2$. Then, in this low energy regime where $|t| \ll M_Z^2$, we find

$$\begin{aligned}
2\,\text{Re}\,\mathcal{X}_{A-\phi} \simeq \frac{1}{4}\sum_{\text{spins}} 2\,\text{Re}\Big[&\frac{-ie^2}{t}\bar{u}(p_2)\gamma_\mu u(p_1)\bar{u}(q_2)\gamma^\mu u(q_1)\times \\
&\times \frac{ig^2\,mM}{M_W^2}\,\bar{u}(q_1)\gamma^5 u(q_2)\Big(-\frac{1}{M_Z^2}\Big)\bar{u}(p_1)\gamma^5 u(p_2)\Big] \\
&= -\frac{8G_F e^2}{2\sqrt{2}}\,\frac{mM}{tM_Z^2}\times \\
&\times \text{Tr}\big[\gamma^\mu(\not{q}_1 + M)\gamma^5(\not{q}_2 + M)\big]\ \text{Tr}\big[\gamma_\mu(\not{p}_1 + m)\gamma^5(\not{p}_2 + m)\big] \\
&= 0\,,
\end{aligned}$$

where M_W is the charged vector boson mass and (3.8) was used.

At this stage, one might also note that in unitary gauge this diagram does not exist, but the same null contribution originates from

the longitudinal part of the Z-boson propagator, which is absent in Feynman gauge ($\xi = 1$).

3.3 ONE-LOOP VIRTUAL CONTRIBUTION

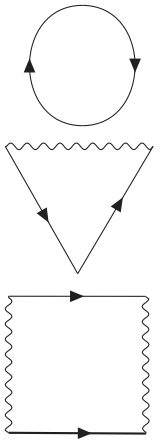

At NLO, in renormalized perturbation theory (RPT), there are three types of diagrams contributing to the cross section of the process.[2] We have one-loop truncated diagrams (see aside) with two, three or four internal lines, which will be analyzed via the Passarino-Veltman (PV) scalar integral decomposition.[3] In fact, we will compute the NLO virtual contribution $\mathcal{X}^{\text{NLO}}$ by considering the interference between these diagrams and the LO one with the photon as propagator:

$$\mathcal{X}^{\text{NLO}} = \frac{1}{4} \sum_{\text{spins}} 2\,\text{Re}[\mathcal{M}_A^* \, \mathcal{M}_{\text{NLO}}] \,,$$

where $\mathcal{M}_{\text{NLO}}$ is the sum of the amplitudes originating from the two-, three- and four-point one-loop diagrams.

We recall how QED is renormalized and its UV divergences are regularized in 3.3.1, self-energy contributions are computed in 3.3.2, vertex correction contributions in 3.3.3 and box contributions in 3.3.4.

We also remark that in RPT the external legs are considered already renormalized. Nevertheless, by the time we will be dealing with the vertex correction, we will also check the Ward Identity (WI) which relates the three-point QED correlator $\langle \overline{\psi} A^\mu \psi \rangle$ with the fermionic two-point correlator $\langle \overline{\psi} \psi \rangle$ in bare perturbation theory (BPT).[4]

3.3.1 *QED renormalization*

Let us first consider the QED quantum action, Γ^Q, originating from the QED classical action:

$$I^Q = \int \mathrm{d}^4x \, \mathcal{L}^Q \,, \quad \mathcal{L}^Q = -\frac{1}{4} F^{\mu\nu} F_{\mu\nu} + \overline{\psi}(\mathrm{i}\partial\!\!\!/ - m - e A\!\!\!/)\psi \,, \qquad (3.13)$$

where $F^{\mu\nu} = \partial^\mu A^\nu - \partial^\nu A^\mu$ is the photon field strength and m is the mass of the fermion whose representation is ψ. Herein, we will not consider the fermion mass term and its renormalization procedure, since the process we are interested in does not involve that part of the lagrangian density.

Since Γ^Q is UV divergent, we have to regularize it. We obtain Γ^Q_ε via the dimensional regularization prescription in $D = 4 - \varepsilon$ dimensions,

2 We will not consider diagrams involving SM massive vector or scalar bosons since they yield a negligible contribution, e.g. much smaller than $\mathcal{X}_{A-Z}$.

3 See appendix B.

4 Field symbols ψ and A^μ were already defined in 2.3.1.

which preserves the gauge invariance of the action. If δ parametrizes the infinitesimal transformation induced by the $U(1)_Q$ gauge group:

$$\varphi' = \varphi + \delta\varphi\,,$$

where $\varphi = \{A, \psi\}$, we may find out how to renormalize the theory by requiring the gauge invariance of the renormalized quantum action, Γ_R^Q:

$$\delta\Gamma_R^Q = 0\,.$$

The lagrangian density in (3.13) already contains all the terms which satisfy the invariance properties required by QED. Then, we rescale the fields and the coupling constant like in the following, aiming to eliminate the UV divergencies:

$$\begin{aligned} A_\mu \to A_\mu^0 &= Z_3^{1/2} A_\mu\,, \\ \psi \to \psi^0 &= Z_2^{1/2}\psi\,, \\ e \to e^0 &= Z_1 Z_2^{-1} Z_3^{-1/2} e\mu^{\varepsilon/2}\,. \end{aligned}$$

As a consequence, we obtain a rescaled lagrangian density:

$$\mathcal{L}_0^Q = -\frac{1}{4}F_0^{\mu\nu}F_{\mu\nu}^0 + \mathrm{i}\overline{\psi}^0(\partial\!\!\!/ + \mathrm{i}e^0 A\!\!\!/^0)\psi^0 \equiv \mathcal{L}^Q + \Delta\mathcal{L}\,,$$

which may be rewritten as

$$\mathcal{L}_0^Q = \mathcal{L}^Q + \frac{1}{4}(1-Z_3)F^{\mu\nu}F_{\mu\nu} - (1-Z_2)\overline{\psi}\mathrm{i}\partial\!\!\!/\psi + e(1-Z_1)\overline{\psi}A\!\!\!/\psi\,.$$

On the other hand, the regularized quantum action may be written in terms of the regularized classical action as in the expansion:[5]

$$\Gamma_\varepsilon^Q = I_\varepsilon + \hbar\left[\frac{1}{\varepsilon}I_1 + I_{\mathrm{fin}}\right] + O(\hbar^2)\,,$$

where $(1/\varepsilon)I_1$ is the one-loop divergent part, while I_{fin} is finite. From

$$\delta\Gamma_\varepsilon^Q = 0$$

it follows that

$$\delta I_1 = \delta I_{\mathrm{fin}} = 0\,.$$

Then, I_1 has to be local in the fields and gauge invariant:

$$I_1 = \int \mathrm{d}^4x\,\mathcal{L}_1\,, \quad \mathcal{L}_1 = \frac{a}{4}F^{\mu\nu}F_{\mu\nu} + c\,\mathrm{i}\overline{\psi}(\partial\!\!\!/ + \mathrm{i}eA\!\!\!/)\psi$$

with a and c finite numerical coefficients defined by:

$$\frac{\hbar}{\varepsilon}\mathcal{L}_1 = -\Delta\mathcal{L}\,,$$

5 We introduced $\hbar$, elsewhere defined to be equal to one, in order to describe properly the quantum action as an $\hbar$-expansion.

which yields the expressions for the counter-terms:

$$Z_3 = 1 + a\frac{\hbar}{\varepsilon}\,, \quad Z_1 = 1 - c\frac{\hbar}{\varepsilon} = Z_2\,.$$

At this stage, as we may safely take the limit $\varepsilon \to 0$, it holds:

$$\Gamma^Q_R = I^Q + \hbar I_{\text{fin}} + O(\hbar^2)\,, \quad \delta\Gamma^Q_R = 0\,,$$

while a and c may be found referring to the QED two- and three-point correlation functions. In particular, assuming to know the results for the vacuum polarization and the vertex correction diagrams, which will be obtained in the following sections, we may give a and c in the on-shell scheme. In fact, by stating the conditions:

$$\Pi(q^2 = 0) = 0\,,$$
$$\Gamma^\mu(q^2 = 0) = \gamma^\mu\,,$$

where Π is the scalar part of the vacuum polarization diagram and q is the 4-momentum entering the loop, one gets:

$$a = -\frac{e^2}{6\pi^2} - \varepsilon\frac{e^2}{12\pi^2}\log\frac{4\pi e^{-\gamma_E}\mu^2}{m^2}\,,$$
$$c = \frac{e^2}{8\pi^2}\left[-1 - \varepsilon\left(\frac{1}{2}\log\frac{4\pi e^{-\gamma_E}\mu^2}{m^2} - \frac{5}{2} - \log\frac{\lambda^2}{m^2}\right)\right]\,,$$

where γ_E is the Euler constant. It is also useful to recall that, in RPT, the counter-terms appear as interactions in the lagrangian density and may be introduced as Feynman diagrams, just like any other interactions. The relevant Feynman rules are quoted in app. A.

3.3.2 *Self Energy*

The unpolarized $O(\alpha^3)$ contribution from self energy diagrams may be represented as in the following:

$\mathcal{X}_2^{\text{NLO}} = \frac{1}{2}\,\text{Re}$ 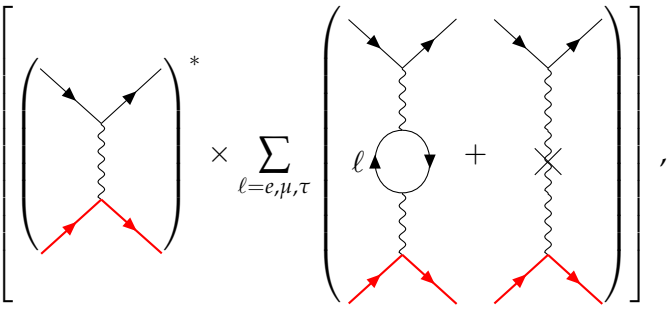 ,

where the sum is meant over an electron, muon and tau bubble, while the cross inserted in the third diagram represents a mass dependent counter-term which makes finite the whole contribution. In fact, the vacuum polarization diagram is logarithmically UV divergent and in

RPT it is necessary to introduce a counter-term to absorb that divergence.

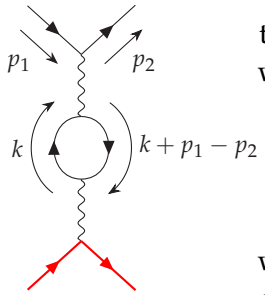

Now, referring ourselves to the diagram aside, we truncate the external legs and make use of the Feynman rules quoted in app. A to write the following amplitude in d dimensions:

$$\Pi^{\mu\nu}(\tau) = -(e\mu^{\frac{\varepsilon}{2}})^2 \int \frac{\mathrm{d}^d k}{(2\pi)^d} \frac{\mathrm{Tr}[\gamma^\mu(\not{k}+m)\gamma^\nu(\not{p}_1-\not{p}_2+m)]}{[k^2-m^2][(k+\tau)^2-m^2]}\,, \tag{3.14}$$

where $\tau \equiv p_1 - p_2$, μ is the 't Hooft dimensional parameter, $\varepsilon = 4-d$ and k is the loop momentum; the iε prescription has been suppressed for brevity. Also, the contributions with a muon or a tau bubble were obtained via the substitutions $m \to M$ and $m \to m_\tau$, respectively.

On the other hand, aiming to subtract the UV divergencies, we used the three counter-terms $\delta_3(m_j)$, $m_j = \{m, M, m_\tau\}$, which are valid in an on-shell scheme:

$$\delta_3(m_j) = -\frac{e^2}{6\pi^2\varepsilon} - \frac{e^2}{12\pi^2}\log\frac{4\pi \mathrm{e}^{-\gamma_E}\mu^2}{m_j^2}\,,$$

with γ_E the Euler constant.

We remark that only at this stage, after subtracting the UV divergencies, it was possible to take the limit $d \to 4$.

These standard QED calculations were carried out either by hand or by the `FeynCalc` code working on `Mathematica`, being both methods based on the PV decomposition. Particularly, the latter firstly decomposes the loop integral in a sum of tensor integrals via the function `TID`, by using a PV basis; then, it reduces the result to PV scalar integrals via `PaVeReduce`, which is what was also done by hand.

Eventually, by substituting (3.14) for the photon propagator in the LO amplitude (3.6), we obtain

$$\begin{aligned}\mathcal{X}_2^{\mathrm{NLO}} = \mathrm{Re}\Big[\frac{8\pi\alpha^3}{3}\sum_{m_j}\Big(&b_1\overline{B}_0(t, m_j^2, m_j^2) + \\ &+ b_2\overline{B}_0(0, m_j^2, m_j^2) + b_3\log m_j + b_0\Big)\Big]\end{aligned} \tag{3.15}$$

where $m_j = \{m, M, m_\tau\}$, the coefficients b_i ($i = 0, \ldots, 3$) are functions of the kinematic invariants, namely m, M, s and t, and their explicit form is quoted in 3.5 together with the two-point PV integrals; $\overline{B}_0$ is the finite part of the two-point PV function:

$$B_0(\ldots) = \frac{2}{\varepsilon} - \log\left(4\pi\mathrm{e}^{-\gamma_E}\mu^2\right) + \overline{B}_0(\ldots)\,.$$

3.3.3 *Vertex Correction*

The unpolarized $O(\alpha^3)$ contribution from vertex correction diagrams may be represented as in the following:

$$\mathcal{X}_3^{\text{NLO}} = \frac{1}{2}\,\text{Re}\left[\quad^{*} \times \sum_{\ell=e,\mu} \quad + \quad\right],$$

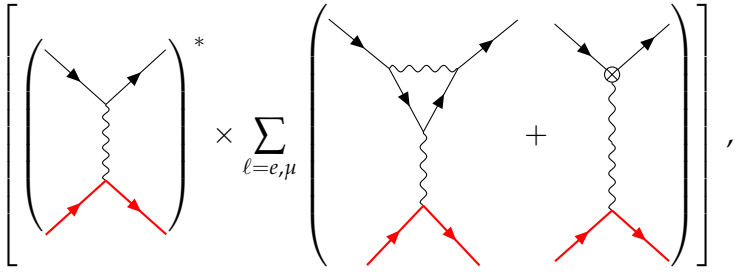

where the sum is meant over an electron and a muon vertex correction, while the crossed dot inserted in the third diagram represents a mass dependent counter-term which makes UV finite the whole contribution. In fact, the vertex correction diagram is logarithmically UV divergent and in RPT it is necessary to introduce a counter-term to absorb that divergence.

Now, referring ourselves to the diagram aside, we truncate all the external legs but those which are stuck to the loop, in order to simplify the expression via the Dirac equation. Then, by making use of the Feynman rules quoted in app. A we write the following amplitude in d dimensions:

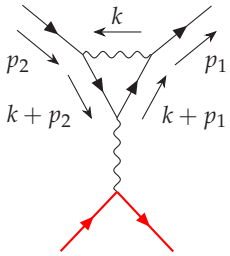

$$\overline{u}_2\Gamma^\mu u_1 = -(e\mu^{\frac{\varepsilon}{2}})^3 \int \frac{\mathrm{d}^d k}{(2\pi)^d} \frac{\overline{u}_2\,\gamma^\rho(\not{p}_2 + \not{k} + m)\gamma^\mu(\not{p}_1 - \not{k} + m)\gamma_\rho\,u_1}{[k^2-\lambda^2][(k+p_1)^2-m^2][(k+p_2)^2-m^2]}, \tag{3.16}$$

where λ is a fictitious mass for the photon, introduced to regularize IR divergences, $\overline{u}_2 \equiv \overline{u}(p_2)$, $u_1 \equiv u(p_1)$ and k is the loop momentum; the $\mathrm{i}\varepsilon$ prescription has been suppressed for brevity. Also, the contribution with a muon triangle was obtained via the substitutions $m \to M$, $p_1 \to q_1$, $p_2 \to q_2$.

On the other hand, aiming to subtract the UV divergencies, we used the two counter-terms $\delta_1(m_k)$, $m_k = \{m, M\}$, which are valid in an on-shell scheme:

$$\delta_1(m_k) = \frac{e^2}{8\pi^2}\left[-\frac{1}{\varepsilon} - \frac{1}{2}\log\frac{4\pi\mathrm{e}^{-\gamma_E}\mu^2}{m_k^2} - \frac{5}{2} - \log\frac{\lambda^2}{m_k^2}\right].$$

We remark that only at this stage, after subtracting the UV divergencies, it was possible to take the limit $d \to 4$, while we have first to sum the LO Bremsstrahlung contribution, before taking $\lambda \to 0$.

As in the vacuum polarization case, these standard QED calculations were carried out either by hand or by `FeynCalc`. Eventually, by

substituting (3.16) for the QED vertex in the LO scattering amplitude (3.6), we obtain

$$\begin{aligned}\mathcal{X}_3^{\text{NLO}} = \text{Re}\Big[\frac{8\pi\alpha^3}{3}\Big(&t_1\overline{B}_0(t,m^2,m^2) + t_2\overline{B}_0(t,M^2,M^2)+\\ &+ t_3\overline{B}_0(0,m^2,m^2) + t_4\overline{B}_0(0,M^2,M^2) + t_5\log\lambda\\ &+ t_6 C_0(m^2,m^2,t;m^2,\lambda^2,m^2) + t_7 C_0(M^2,M^2,t;M^2,\lambda^2,M^2)+\\ &+ t_8\{\log m + \log M\} + t_0\Big)\Big]\,,\end{aligned} \tag{3.17}$$

where the coefficients t_i ($i = 0,\dots,8$) are functions of the kinematic invariants and their explicit form is quoted in 3.5 together with the two- and three-point PV integrals.

Ward Identity

Moreover, as we mentioned earlier, we dedicate the following paragraph to the WI existing between the 3-point and the fermionic 2-point QED correlators. In particular, we switch to BPT and consider the one-loop contributions to those Green functions, also recalled as vertex correction and wave function renormalization, respectively.

A direct consequence from WI is

$$\text{UV}\,[Z_1] + 2\text{UV}\,[Z_2]^{1/2} = 0 \quad \text{order by order}\,,$$

where UV $[x]$ means UV divergent part of x. Therefore, by using the standard result for Z_2 and the above mentioned result for Z_1, where $Z_2 \equiv 1+\delta_2$ renormalizes the wave function and $Z_1 \equiv 1+\delta_1$ the vertex, we found that the identity is satisfied at one-loop.

3.3.4 *Box*

The unpolarized $O(\alpha^3)$ contribution from box diagrams may be represented as in the following:

$$\mathcal{X}_4^{\text{NLO}} = \frac{1}{2}\,\text{Re}\left[\sum_{\parallel,\times}\right.$$
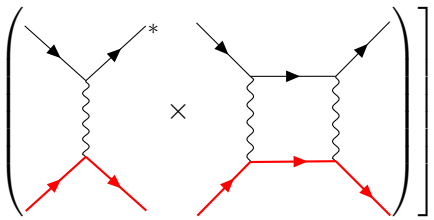
$$\left.\right]\,,$$

where the sum is meant over a box diagram ($\parallel$) with the internal photon lines like in the figure and a (crossed) box diagram ($\times$) with crossed internal photon lines and identical fermionic lines.

One may note that, inverting for example the arrows on the muon line, the crossed diagram turns out to be identical to the direct one, if an overall minus sign is added before the crossed diagram and the following substitution is done, on the crossed diagram alike:

$$u = 2M^2 + 2m^2 - s - t \to s\,.$$

Then, a valid check for our calculations was a comparison between the direct diagram ($\|$) and the crossed one ($\times$), as in the following diagrammatic representation:

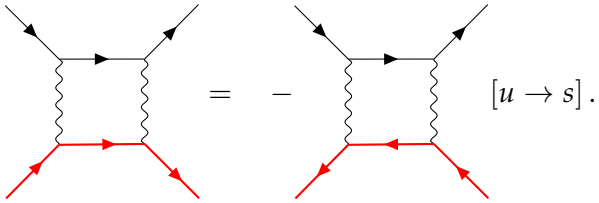

Referring ourselves to the diagram aside, we keep all the external legs in order to simplify the expression via the Dirac equation. Then, by making use of the Feynman rules quoted in app. A we write the following amplitude in 4 dimensions since the diagram is not UV divergent, as one may easily note by a dimensional analysis:

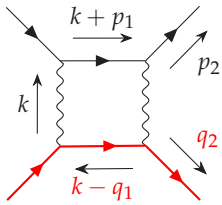

$$B_{\|} = e^4 \int \frac{\mathrm{d}^4k}{(2\pi)^4} \frac{\overline{u}_{2e}\,\gamma^\sigma(\not{k}+\not{p}_1+m)\gamma^\rho\,u_{1e}\,\overline{u}_{2\mu}\,\gamma_\sigma(\not{k}-\not{q}_1+M)\gamma_\rho\,u_{1\mu}}{[k^2-\lambda^2][(k+p_1)^2-m^2][(k+\tau)^2-\lambda^2][(k-q_1)^2-M^2]}\,, \tag{3.18}$$

where $\overline{u}_{2i} \equiv \overline{u}(p_{2i})$, $u_{1i} \equiv u(p_{1i})$ $(i = e, \mu)$ and k is the loop momentum; the iε prescription has been suppressed for brevity.

Then, the contribution $B_\times$ from the crossed box was obtained via the substitutions $p_1 \to -p_2$, $p_2 \to -p_1$ applied to the whole expression of $B_{\|}$ but the spinors. We also remark that we have first to sum the LO Bremsstrahlung contribution, before taking $\lambda \to 0$ in both cases, like with the vertex correction.

In this case the computation was done only by `FeynCalc` and aiming to simplify its work, we exploited the ultraviolet finiteness of the box diagrams. In fact, in order to use the Dirac equation and contract the Lorentz indices, we first contracted the amplitude (3.18) with the LO one (3.6) and then we solved the loop integral in terms of PV scalar integrals. The correctness of this procedure is guaranteed by the UV finiteness of the diagrams.

Eventually we obtain

$$\begin{aligned}
\mathcal{X}_4^{\mathrm{NLO}} = \mathrm{Re}\Big[\frac{8\pi\alpha^3}{3}\Big(&s_1\overline{B}_0(0,m^2,m^2) + s_2\overline{B}_0(0,M^2,M^2) + s_3\overline{B}_0(t,0,0) + \\
&+ s_4\overline{B}_0(0,m^2,M^2) + s_5\overline{B}_0(s,m^2,M^2) + s_6\overline{B}_0(u,m^2,M^2) + \\
&+ s_7 C_0(m^2,M^2,s;m^2,\lambda^2,m^2) + s_8 C_0(m^2,M^2,u;M^2,\lambda^2,M^2) + \\
&+ s_9 C_0(m^2,m^2,t;\lambda^2,m^2,\lambda^2) + s_{10} C_0(M^2,M^2,t;\lambda^2,M^2,\lambda^2) + \\
&+ s_{11} D_0(m^2,m^2,M^2,M^2,t,s;\lambda^2,m^2,\lambda^2,M^2) + \\
&+ s_{12} D_0(m^2,m^2,M^2,M^2,t,u;\lambda^2,m^2,\lambda^2,M^2) + s_0\Big)\Big]\,,
\end{aligned} \tag{3.19}$$

where the coefficients s_i ($i = 0, \dots, 12$) are functions of the kinematic invariants and their explicit form is quoted in 3.5 together with the two-, three- and four-point PV integrals.

3.4 BREMSSTRAHLUNG CONTRIBUTION

In the previous section we obtained a one-loop virtual contribution to the muon-electron cross section which is UV finite. However, the results still contain IR divergences, at this stage regularized by the fictitious photon mass λ: as $\lambda \to 0$ we immediately get a singularity.

The recipe one follows to solve this issue is the Bloch-Nordsieck prescription, which asserts that the cross section will be IR finite if soft Bremsstrahlung diagrams at LO are summed to the virtual contribution. In particular, we consider soft photon emission both in the initial and in the final state, namely emission of photons with an energy in the lab frame less than ω, where ω is the sensibility threshold of the experimental setup. Then, IR divergencies which are opposite to the virtual one will show up and cancel the latter.

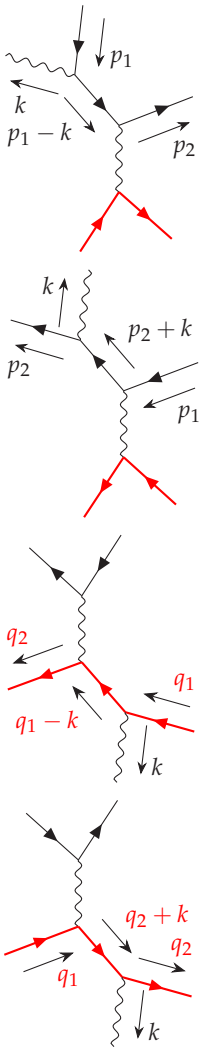

The calculation of the LO Bremsstrahlung amplitudes was carried out by hand, closely following the approach proposed by 't Hooft and Veltman in (*58*).

Now, referring ourselves to the four soft emission diagrams aside, being $k = (k^0, \mathbf{k})$ the soft photon 4-momentum and λ its fictional mass, we may write the relevant amplitude by factorizing the LO amplitude (3.6):

$$\mathcal{X}_\omega^{\mathrm{LO}} = -\mathcal{X}_A\, e^2 \int^{k^0<\omega} \frac{\mathrm{d}^3\mathbf{k}}{(2\pi)^3 2k^0} \left|\mathcal{E}(p_1, p_2, q_1, q_2, k)\right|^2 , \tag{3.20}$$

where

$$\mathcal{E}(p_1, p_2, q_1, q_2, k) = -\frac{p_1}{p_1 \cdot k} + \frac{p_2}{p_2 \cdot k} - \frac{q_1}{q_1 \cdot k} + \frac{q_2}{q_2 \cdot k} .$$

This result was obtained by using the customary Feynman rules. In particular, for example from the first diagram, we get the following amplitude:

$$\mathcal{M}_1 = \frac{\mathrm{i}e^3}{t} \overline{u}(p_2)\gamma^\mu \frac{\not{p}_1 + \not{k} + m}{(p_1 - k)^2 - m^2} \not{\epsilon} u(p_1) \overline{u}(q_2)\gamma_\mu u(q_1) .$$

Since we may neglect $\not{k}$ and λ^2 with respect to $\not{p}_1$ and m^2, being the photon soft, and by using the Clifford algebra $\{\gamma^\mu, \gamma^\nu\} = 2g^{\mu\nu}$ and the Dirac equation, we find

$$\mathcal{M}_1 = \left[\frac{\mathrm{i}e^2}{t} \overline{u}(p_2)\gamma^\mu u(p_1) \overline{u}(q_2)\gamma_\mu u(q_1)\right] e \frac{p_1 \cdot \epsilon}{-p_1 \cdot k} .$$

At this stage it is easy to see how (3.20) was obtained by taking the absolute square of $\mathcal{M}_1$, also recalling that: (i) the sum over polarizations, in the approximation of a photon without a fictional mass, yields

$$\sum_{\text{pol's}} \epsilon^\alpha \epsilon^\beta = -g^{\alpha\beta}$$

(ii) the recoil of the fermion by the emitted photon is neglected (then, there is no k in the 4-momentum conservation δ) and (iii) the integral over $\mathbf{k}$ shows up as a phase space factor, like we saw in (3.3). Clearly, the other three diagrams yield similar contributions, calculable via the substitutions ($p_1 \to p_2$, $k \to -k$), ($p_1 \to q_1$) and ($p_1 \to q_2$, $k \to -k$), respectively.

Now we turn to the calculation of the integrals in (3.20). In particular they show up in the following form:

$$\mathcal{I}(p_i, p_j) = \int^{k^0<\omega} \frac{\mathrm{d}^3\mathbf{k}}{k^0} \frac{1}{(p_i \cdot k)(p_j \cdot k)},$$

where $p_i, p_j \equiv \{p_1, p_2, q_1, q_2\}$. Then, in the lab frame,[6]

$$\begin{aligned}\mathcal{X}_\omega^{LO} = -\mathcal{X}_A \frac{4\pi\alpha}{2(2\pi)^3} \Big[& 2m^2 \mathcal{I}(p_1, p_1) + 2M^2 \mathcal{I}(q_1, q_1) - \\ & - 2\Big(m^2 - \frac{t}{2}\Big) \mathcal{I}(p_1, p_2) - 2\Big(M^2 - \frac{t}{2}\Big) \mathcal{I}(q_1, q_2) + \\ & + 4\frac{1}{2}(s - m^2 - M^2)\, \mathcal{I}(q_1, p_1) - 4\frac{1}{2}(m^2 + M^2 - u)\, \mathcal{I}(q_1, p_2) \Big].\end{aligned} \tag{3.21}$$

The integrals with $p_i = p_j$ yield a direct calculation, while in the other cases the procedure is more articulate and we follow 't Hooft and Veltman (58). Anyway, the calculations are briefly quoted in app. B while for the results in section 3.5 we will keep the implicit form in terms of the $\mathcal{I}(p_i, p_j)$ integrals.

Here we only sketch the IR divergencies cancellation between one-loop virtual diagrams and real LO Bremsstrahlung diagrams, which has been successfully verified by noting that the following sums are IR finite:

- Electron vertex correction:

$$\begin{aligned}& \mathrm{Re}\Big[\frac{8\pi\alpha^3}{3}\Big(\frac{t_5}{2}\log\lambda + t_6 C_0(m^2, m^2, t; m^2, \lambda^2, m^2)\Big)\Big] - \\ & - \mathcal{X}_A \frac{e^2}{2(2\pi)^3}\Big[2m^2 \mathcal{I}(p_1, p_1) - 2\Big(m^2 - \frac{t}{2}\Big)\mathcal{I}(p_1, p_2)\Big]\end{aligned}$$

6 Symmetries between *a priori* different integrals will be more clear in appendix B.

- Muon vertex correction:

$$\mathrm{Re}\Big[\frac{8\pi\alpha^3}{3}\Big(\frac{t_5}{2}\log\lambda + t_7 C_0(M^2, M^2, t; M^2, \lambda^2, M^2)\Big)\Big] - \\ - \mathcal{X}_A \frac{e^2}{2(2\pi)^3}\Big[2M^2\,\mathcal{I}(q_1, q_1) - 2\Big(M^2 - \frac{t}{2}\Big)\,\mathcal{I}(q_1, q_2)\Big]$$

- Direct box:

$$\mathrm{Re}\Big[\frac{8\pi\alpha^3}{3}\Big(s_{11} D_0(m^2, m^2, M^2, M^2, t, s; \lambda^2, m^2, \lambda^2, M^2) + \\ + s_7 C_0(m^2, M^2, s; m^2, \lambda^2, M^2)\Big)\Big] - \\ - \mathcal{X}_A \frac{e^2}{2(2\pi)^3}\Big[4\frac{1}{2}(s - m^2 - M^2)\,\mathcal{I}(q_1, p_1)\Big]$$

- Crossed box:

$$\mathrm{Re}\Big[\frac{8\pi\alpha^3}{3}\Big(s_{12} D_0(m^2, m^2, M^2, M^2, t, u; \lambda^2, m^2, \lambda^2, M^2) + \\ + s_8 C_0(m^2, M^2, u; m^2, \lambda^2, M^2)\Big)\Big] - \\ - \mathcal{X}_A \frac{e^2}{2(2\pi)^3}\Big[-4\frac{1}{2}(m^2 + M^2 - u)\,\mathcal{I}(q_1, p_2)\Big]$$

At this stage, we may safely take the limit $\lambda \to 0$ and give the final results in the following section. We remark that $C_0(m^2, m^2, t; \lambda^2, m^2, \lambda^2)$ and $C_0(M^2, M^2, t; \lambda^2, M^2, \lambda^2)$, showing up in the box contributions, are already IR finite, differently from all the other three- and four-point PV functions (59).

3.5 RESULTS

Once UV and IR divergencies have been canceled, we may give the final result for the $\mu^- e^-$ elastic scattering differential cross section at order α^3 (i.e. at NLO).

Though, before writing it, we would like to quote the modifications by which the result is affected, if we change a particle with an antiparticle in the initial or in the final state. In fact, the prescription follows straightforward: every time μ^- is replaced by μ^+ or e^- by e^+, the box contributions, $\mathcal{I}(p_1, q_1)$ and $\mathcal{I}(p_1, q_2)$ take a on overall minus sign, while LO contributions, self energies and vertex corrections remain the same.

Now, it is clear from the previous sections that, at order α^3,

$$\Big(\frac{\mathrm{d}\sigma}{\mathrm{d}t}\Big)^{\mathrm{NLO}}_{\mu^- e^- \to \mu^- e^-} = -\frac{\mathcal{X}}{16\pi\Lambda(s, m^2, M^2)}\,, \tag{3.22}$$

where

$$\mathcal{X} = \mathcal{X}_A + \mathcal{X}_2^{\mathrm{NLO}} + \mathcal{X}_3^{\mathrm{NLO}} + \mathcal{X}_4^{\mathrm{NLO}} + \mathcal{X}_\omega^{\mathrm{LO}}\,.$$

This is the final expression we get. We recall that it is a function of the kinematic invariants (m, M, s and t) and the sensitivity threshold in energy of the experimental setup, ω.

$\mathcal{X}_A$, $\mathcal{X}_2^{\text{NLO}}$, $\mathcal{X}_3^{\text{NLO}}$, $\mathcal{X}_4^{\text{NLO}}$, $\mathcal{X}_\omega^{\text{LO}}$ are respectively quoted in (3.6), (3.15), (3.17), (3.19) and (3.21), while in the following we quote the explicit form of the coefficients b_i, t_i and s_i. Also, in appendix B we quote the relevant PV functions and the Bremsstrahlung integrals.

For every scalar integral appearing in the differential cross section, the relevant coefficients are listed:

- $\overline{B}_0(t, m^2, m^2)$:

$$
\begin{aligned}
&b_1 + t_1 = \\
&= \frac{1}{t^3\,(t-4m^2)}\Big[128m^2t\left(-s\left(m^2+2M^2\right)+\left(m^2+M^2\right)^2+s^2\right)+ \\
&+4t^3\left(22m^2-13s\right)+4t^2\big(3m^4+m^2\left(58s-14M^2\right)-13(M^2- \\
&-s)^2\big)+128m^4\left(m^2+M^2-s\right)^2-26t^4\Big]
\end{aligned}
$$

- $\overline{B}_0(t, M^2, M^2)$:

$$
\begin{aligned}
&b_1 + t_2 = \\
&= 2\Big[\frac{1}{t^2\,(t-4M^2)}\Big(48M^2\left(m^2+M^2-s\right)^2-6t\big(3m^4+2m^2\big(M^2- \\
&-3s\big)+3M^4-14M^2s+3s^2\big)+18t^2\left(2M^2-s\right)-9t^3\Big)- \\
&-\Big(4\left(2M^2+t\right)\left(2\left(m^2+M^2-s\right)^2+2st+t^2\right)\Big)\Big]
\end{aligned}
$$

- $\overline{B}_0(t, m_\tau^2, m_\tau^2)$:

$$
b_1 = \frac{8}{t^3}\left(2m_\tau^2+t\right)\left(2\left(m^2+M^2-s\right)^2+2st+t^2\right)
$$

- $\overline{B}_0(0, m^2, m^2)$:

$$
\begin{aligned}
&b_2 + t_3 + s_1 = \\
&\frac{1}{t^2}\left(-8s\left(5m^2+9M^2\right)+36\left(m^2+M^2\right)^2+36s^2\right)+ \\
&+\frac{32m^2\left(m^2+M^2-s\right)^2}{t^3}\frac{3\left(m^2-M^2+s\right)\left(9m^2-M^2+s\right)}{m^2\left(t-4m^2\right)}+ \\
&+\frac{24\left(2m^4-3m^2\left(M^2+s\right)+\left(M^2-s\right)^2\right)}{m^4-2m^2\left(M^2+s\right)+\left(M^2-s\right)^2}+ \\
&+\frac{34m^8-4m^6\left(11M^2+14s\right)+m^4\left(-23M^4-170M^2s+s^2\right)}{m^2t\left((m-M)^2-s\right)\left((m+M)^2-s\right)}+ \\
&+\frac{12m^2\left(M^2-s\right)^2\left(3M^2+2s\right)-3\left(M^2-s\right)^4}{m^2t\left((m-M)^2-s\right)\left((m+M)^2-s\right)}+ \\
&+\frac{12m(m+M)}{(m-M)^2-s-t}+\frac{12m(m-M)}{(m+M)^2-s-t}
\end{aligned}
$$

- $\overline{B}_0(0, M^2, M^2)$:

$$
\begin{aligned}
&b_2 + t_4 + s_2 = \\
&\frac{-8s\left(9m^2+5M^2\right)+36\left(m^2+M^2\right)^2+36s^2}{t^2}+ \\
&+\frac{32M^2\left(m^2+M^2-s\right)^2}{t^3}+\frac{3\left(-m^2+M^2+s\right)\left(-m^2+9M^2+s\right)}{M^2\left(t-4M^2\right)}+ \\
&+\frac{-3m^8+12m^6\left(3M^2+s\right)-m^4\left(23M^4+48M^2s+18s^2\right)}{M^2t\left((m-M)^2-s\right)\left((m+M)^2-s\right)}- \\
&-\frac{4m^2\left(11M^6+41M^4s+3M^2s^2-3s^3\right)}{M^2t\left((m-M)^2-s\right)\left((m+M)^2-s\right)}+ \\
&+\frac{\left(M^2-s\right)^2\left(34M^4+18M^2s-3s^2\right)}{M^2t\left((m-M)^2-s\right)\left((m+M)^2-s\right)}+ \\
&+\frac{12M(m+M)}{(m-M)^2-s-t}+\frac{12M(M-m)}{(m+M)^2-s-t}+ \\
&+12\left(\frac{M(M-m)}{(m-M)^2-s}+\frac{M(m+M)}{(m+M)^2-s}+2\right)
\end{aligned}
$$

- $\overline{B}_0(0, m_\tau^2, m_\tau^2)$:

$$b_2 = \frac{16m_\tau^2}{t^3}\left(2\left(m^2+M^2-s\right)^2+2st+t^2\right)$$

- $\overline{B}_0(t, 0, 0)$:

$$s_3 = \frac{12(4mM-t)(4mM+t)\left(2\left(m^2+M^2-s\right)-t\right)}{t\left(4m^2-t\right)\left(t-4M^2\right)}$$

- $\overline{B}_0(0, m^2, M^2)$:

$$s_4 = \frac{12(4mM-t)(4mM+t)\left(2\left(m^2+M^2-s\right)-t\right)}{t\left(4m^2-t\right)\left(t-4M^2\right)}$$

- $\overline{B}_0(s, m^2, M^2)$:

$$
\begin{aligned}
s_5 = &-12\Bigg(\frac{m^6+m^4\left(-M^2-3s+t\right)-m^2\left(M^4+2M^2(s+t)-3s^2\right)}{t\left((m-M)^2-s\right)\left((m+M)^2-s\right)}+ \\
&+\frac{t\left(M^4-s^2\right)+\left(M^2-s\right)^3}{t\left((m-M)^2-s\right)\left((m+M)^2-s\right)}\Bigg)
\end{aligned}
$$

- $\overline{B}_0(u, m^2, M^2)$:

$$s_6 = 12\left(-\frac{m^2+M^2-s}{t}-\frac{(m-M)^2}{(m+M)^2-s-t}+\frac{(m+M)^2}{-(m-M)^2+s+t}\right)$$

- $C_0(m^2, m^2, t; m^2, \lambda^2, m^2)$:

$$t_6 = \frac{12}{t^2}\left(2m^2-t\right)\left(2\left(m^2+M^2-s\right)^2+2st+t^2\right)$$

- $C_0(M^2, M^2, t; M^2, \lambda^2, M^2)$:

$$t_7 = \frac{12}{t^2}\left(2M^2 - t\right)\left(2\left(m^2 + M^2 - s\right)^2 + 2st + t^2\right)$$

- $C_0(m^2, M^2, s; m^2, \lambda^2, M^2)$:

$$s_7 = -\frac{12}{t}(2s + t)\left(m^2 + M^2 - s\right)t$$

- $C_0(m^2, M^2, u; m^2, \lambda^2, M^2)$:

$$s_8 = -\frac{12}{t}\left(4m^2 + 4M^2 - 2s - t\right)\left(m^2 + M^2 - s - t\right)$$

- $C_0(m^2, m^2, t; \lambda^2, m^2, \lambda^2)$:

$$s_9 = \frac{12}{t\left(4m^2 - t\right)}\left(8m^4 - 8m^2t + t^2\right)\left(2\left(m^2 + M^2 - s\right) - t\right)$$

- $C_0(M^2, M^2, t; \lambda^2, M^2, \lambda^2)$:

$$s_{10} = \frac{12}{t\left(4M^2 - t\right)}\left(8M^4 - 8M^2t + t^2\right)\left(2\left(m^2 + M^2 - s\right) - t\right)$$

- $D_0(m^2, m^2, M^2, M^2, t, s; \lambda^2, m^2, \lambda^2, M^2)$:

$$s_{11} = -\frac{6}{t}\left(m^2 + M^2 - s\right)\left(4\left(m^2 + M^2 - s\right)^2 + 2st + t^2\right)$$

- $D_0(m^2, m^2, M^2, M^2, t, u; \lambda^2, m^2, \lambda^2, M^2)$:

$$s_{12} = -\frac{6}{t}\left(m^2 + M^2 - s - t\right)\left(-2t\left(2\left(m^2 + M^2\right) - 3s\right) + \right.$$
$$\left. + 4\left(m^2 + M^2 - s\right)^2 + 3t^2\right)$$

- $\log m$, $\log M$:

$$b_3 + t_8 = \frac{20\left(2\left(m^2 + M^2 - s\right)^2 + 2st + t^2\right)}{t^2}$$

- $\log m_\tau$:

$$b_3 = -\frac{16\left(2\left(m^2 + M^2 - s\right)^2 + 2st + t^2\right)}{t^2}$$

- $\log \lambda$:

$$t_5 = -\frac{48\left(2\left(m^2 + M^2 - s\right)^2 + 2st + t^2\right)}{t^2}$$

- $b_0 + t_0 + s_0 =$

$$
\begin{aligned}
&- 48s^2\left(m^2+M^2\right) - 816\left(m^2-M^2\right)^2\left(m^2+M^2\right) - \\
&- \frac{384M^4\left(-m^2+M^2+s\right)\left(-m^2+9M^2+s\right)}{t-4M^2} - \\
&- \frac{16t^3\left(-7s\left(m^2+M^2\right)+5\left(m^2-M^2\right)^2+2s^2\right)}{m^4-2m^2\left(M^2+s\right)+\left(M^2-s\right)^2} - \\
&- \frac{384m^4\left(m^2-M^2+s\right)\left(9m^2-M^2+s\right)}{t-4m^2} - \\
&- 16t\left(13m^4+13s\left(m^2+M^2\right)-22m^2M^2+13M^4+4s^2\right) - \\
&- 96s\left(11m^4-6m^2M^2+11M^4\right) - \\
&- \frac{24(m+M)^2\left((m-M)^2-s\right)^3}{(m-M)^2-s-t} - \\
&- \frac{24(m-M)^2\left((m+M)^2-s\right)^3}{(m+M)^2-s-t} + \\
&+ \left[\frac{-45m^6+m^4\left(45M^2+32s\right)+m^2\left(M^2+7s\right)\left(45M^2+11s\right)}{m^4-2m^2\left(M^2+s\right)+\left(M^2-s\right)^2} - \right. \\
&\left. - \frac{\left(M^2-s\right)^2\left(45M^2+64s\right)}{m^4-2m^2\left(M^2+s\right)+\left(M^2-s\right)^2}\right]t^2
\end{aligned}
$$

4

CONCLUSIONS

After reviewing the state of the art about the SM theoretical prediction for the anomalous magnetic moment of the muon, we computed the $\mu - e$ elastic scattering differential cross section at NLO in QED.

This very process was chosen in the framework of a recent proposal, MUonE, for calculating the LO hadronic contribution to a_μ. In fact, it aims to measure the running of α in a space-like region by scattering muons on atomic electrons through the elastic process $\mu\, e \to \mu\, e$. The differential cross section of the latter, measured as a function of the squared 4-momentum transfer $t < 0$, provides direct sensitivity to the LO hadronic contribution to a_μ.

The radiative corrections to the $\mu - e$ elastic scattering differential cross section were computed long time ago and revisited more recently. As a first check, we recalculated these corrections and found perfect agreement with the latest result in literature, both for the virtual corrections and for the soft photon emission, although unsolved integrals still show up in the final expressions of that reference. We found out that some of the pioneering publications contain typos or errors, so that they cannot be directly employed. Then, aim of this work is to obtain a correct and usable result, which may be directly tested or used by experiments.

The differential cross section was calculated via the PV scalar integral decomposition, which is also encoded in the `FeynCalc` routine. The final result is given in its most explicit form, as a function of the kinematic invariants and the sensitivity threshold in energy of the experimental setup, as small as the regime of soft photon emission requires. A crucial test which the result passed was the request to be IR finite, via the cancellation of the IR divergencies appearing both in three- and four-point PV functions and in Bremsstrahlung integrals. In fact, the divergencies, at first regularized by a cut-off, canceled out exactly.

Then, the result shall be directly used by experiments like MUonE. The aim of that experiment will be the ambitious goal of measuring the differential cross section of the process with an accuracy of 10 ppm. This requires, on the theoretical side, the knowledge of the

QED radiative corrections at NNLO, and this thesis has been a first step toward this direction. In parallel to this work, in (60), the master integrals for the two-loop, planar box-diagrams, are evaluated, adopting the method of differential equations and the Magnus exponential series. The evaluation of the missing contributions, due to non-planar box graphs, will be the subject of a future work.

Eventually, we recall that these calculations turn out to be also relevant for crossing-related processes, such as di-muon production at e^+e^- colliders, as well as for the QCD corrections to top-pair production at hadron colliders.

A

CONVENTIONS – USEFUL IDENTITIES

$$c = \hbar = 1$$

METRIC

$$g = \text{diag}(1, -1, -1, -1)$$

DIRAC MATRICES IDENTITIES IN 4-DIM

$$\begin{aligned}
\{\gamma^\mu, \gamma^\nu\} &= 2g^{\mu\nu} \qquad \text{(Clifford 4-algebra)} \\
\{\gamma^\mu, \gamma^5\} &= 0 \\
\gamma^\mu\gamma_\mu &= 4\mathbb{1}_4 \\
\gamma^\mu\gamma^\nu\gamma_\mu &= -2\gamma^\nu \\
\gamma^\mu\gamma^\nu\gamma^\rho\gamma_\mu &= 4g^{\nu\rho} \\
\text{Tr}[\text{odd number of } \gamma\text{'s}] &= 0 \\
\text{Tr}[\gamma^\mu\gamma^\nu] &= 4g^{\mu\nu} \\
\text{Tr}[\gamma^\mu\gamma^\nu\gamma^\rho\gamma^\sigma] &= 4(g^{\mu\nu}g^{\rho\sigma} - g^{\mu\rho}g^{\nu\sigma} + g^{\mu\sigma}g^{\nu\rho}) \\
\text{Tr}\big[(0 \text{ to } 3\gamma\text{'s})\gamma^5\big] &= 0 \\
\text{Tr}\big[\gamma^\mu\gamma^\nu\gamma^\rho\gamma^\sigma\gamma^5\big] &= -4i\varepsilon^{\mu\nu\rho\sigma}
\end{aligned}$$

DIRAC MATRICES IDENTITIES IN d-DIM

$$\begin{aligned}
\gamma_\mu\gamma^\nu\gamma^\mu &= (2-d)\gamma^\nu \\
\gamma_\mu\gamma^\nu\gamma^\rho\gamma^\mu &= 4g^{\nu\rho} + (d-4)\gamma^\nu\gamma^\rho \\
\gamma_\mu\gamma^\nu\gamma^\rho\gamma^\sigma\gamma^\mu &= -2\gamma^\sigma\gamma^\rho\gamma^\nu + (4-d)\gamma^\nu\gamma^\rho\gamma^\sigma
\end{aligned}$$

FEYNMAN RULES IN $\xi = 1$ GAUGE

- External lines:

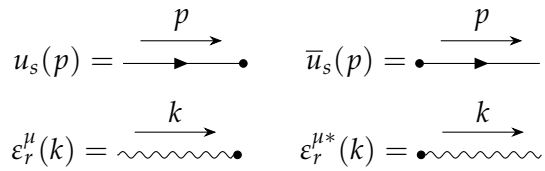

  where p and k are the fermion and photon 4-momenta, respectively, while s is the fermion spin and r the photon polarization.

- Internal lines:

$$= \frac{\mathrm{i}(\not{p} + m)}{p^2 - m^2 + \mathrm{i}\varepsilon}$$

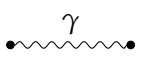
$$= \frac{-\mathrm{i}g^{\mu\nu}}{k^2 + \mathrm{i}\varepsilon}$$

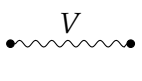
$$= \frac{-\mathrm{i}g^{\mu\nu}}{k^2 - M_V^2 + \mathrm{i}\varepsilon}$$

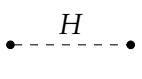
$$= \frac{\mathrm{i}}{k^2 - M_H^2 + \mathrm{i}\varepsilon}$$

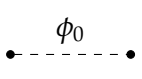
$$= \frac{\mathrm{i}}{k^2 - M_Z^2 + \mathrm{i}\varepsilon}$$

  where p and k are the fermion and boson 4-momenta, m is the mass of a fermion, M_V is the mass of a vector boson (W or Z), M_H and M_Z are the Z- and Higgs boson masses, respectively.

- QED vertex:

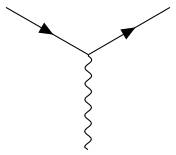
$$= -\mathrm{i}e\gamma^\mu$$

  In this thesis we take $e > 0$.

- Fermion-Higgs interaction:

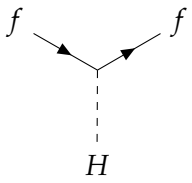

$$= -\frac{\mathrm{i}g}{2}\frac{m_f}{M_W}\gamma^5$$

  where M_W is the charged vector boson mass.

- Fermion-Goldstone interaction:

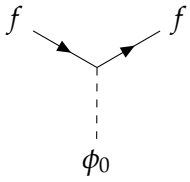

$$= g\frac{m_f}{M_W}\gamma^5$$

- QED counter-terms (on-shell scheme, dim. reg.):

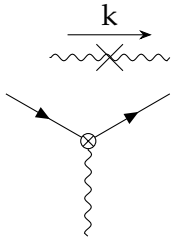

$$= -\mathrm{i}\,\delta_3(m_i)k^2 g^{\mu\nu}$$

$$= -\mathrm{i}e\,\delta_1(m_i)\gamma^\mu$$

where

$$\delta_3(m_i) = -\frac{e^2}{6\pi^2\varepsilon} - \frac{e^2}{12\pi^2}\log\frac{4\pi e^{-\gamma_E}\mu^2}{m_i^2}$$
$$\delta_1(m_i) = \frac{e^2}{8\pi^2}\Big[-\frac{1}{\varepsilon} - \frac{1}{2}\log\frac{4\pi e^{-\gamma_E}\mu^2}{m_i^2} - \frac{5}{2} - \log\frac{\lambda^2}{m_i^2}\Big]$$

with $\varepsilon = 4 - d$, γ_E is the Euler constant, μ the 't Hooft dimensional parameter, m_i the mass of the relevant particle, λ a fictional photon mass introduced to regularize IR divergencies.

B

SCALAR INTEGRALS

In this appendix we will briefly describe how one usually copes with one-loop integrals, whose relevance in this thesis is clear. In fact, except for the self energy type of diagrams, the standard integration over the Feynman parameters is normally quite difficult.

The first approach to overcome this issue was that of Passarino and Veltman (*61*). They considered a general one-loop tensor integral like

$$\frac{(2\pi\mu)^{4-d}}{\mathrm{i}\pi^2}\int \mathrm{d}^d k\,\frac{k^{\mu_1}\dots k^{\mu^p}}{D_0 D_1 D_2 \dots D_{n-1}}\,,$$

where

$$D_i = (k+r_i)^2 - m_i^2 + \mathrm{i}\varepsilon$$

and the internal momenta r_i are related to the external momenta (all taken to be incoming) via:

$$\begin{aligned} r_j &= \sum_{i=1}^{j} p_i\,, \qquad (j=1,\dots,n-1)\\ r_0 &= \sum_{i=1}^{n} p_i = 0\,. \end{aligned}$$

Further, they noticed that the tensor integral may be decomposed in a basis of four scalar integrals:

$$\begin{aligned} A_0(m^2) &= \frac{(2\pi\mu)^{\varepsilon}}{\mathrm{i}\pi^2}\int \mathrm{d}^d k\,\frac{1}{k^2-m_0^2}\\ B_0(r_{10}^2; m_0^2, m_1^2) &= \frac{(2\pi\mu)^{\varepsilon}}{\mathrm{i}\pi^2}\int \mathrm{d}^d k\,\prod_{i=0}^{1}\frac{1}{(k+r_i)^2-m_i^2}\\ C_0(r_{10}^2, r_{12}^2, r_{20}^2; \dots) &= \frac{(2\pi\mu)^{\varepsilon}}{\mathrm{i}\pi^2}\int \mathrm{d}^d k\,\prod_{i=0}^{2}\frac{1}{(k+r_i)^2-m_i^2}\\ D_0(r_{10}^2, r_{12}^2, r_{20}^2, r_{30}^2, r_{13}^2, r_{23}^2; \dots) &= \frac{(2\pi\mu)^{\varepsilon}}{\mathrm{i}\pi^2}\int \mathrm{d}^d k\,\prod_{i=0}^{3}\frac{1}{(k+r_i)^2-m_i^2}\,, \end{aligned} \tag{B.1}$$

where $r_{\mathrm{ij}}^2 = (r_i - r_j)^2$, the dots in the integral arguments are meant as the squared masses and the $\mathrm{i}\varepsilon$ prescription was suppressed for brevity.

Also, it can be shown that these are the only four independent integrals into which one may decomposes the general one-loop integral.

A reader interested in the decomposition is demanded to (61), while here we will quote some of the calculation techniques useful to solve the integrals in (B.1), strictly following 't Hooft and Veltman (58).

ONE-POINT FUNCTION We did not use the one-point function A_0 in our decomposition since one may get:

$$A_0(m^2) = m^2[1 + B_0(0; m^2, m^2)]\,. \tag{B.2}$$

As a result, our decomposition includes two-, three- and four- point functions only. Every time a one-point function was found by the `FeynCalc` code, it was rewritten in terms of a two-point function via (B.2).

TWO-POINT FUNCTION The two-point function B_0 does not present any particular computation difficulty if it is solved by introducing a Feynman parameter. This lets the product of the two denominators become a single squared polynomial in the loop momentum. Thus, the integration over the latter becomes straightforward as a logarithm and the integration of the Feynman parameter is carried out in terms of the roots of the logarithm polynomial argument.

Standard results in a dimensional regularization framework, compatible with our conventions, may be found in (59), section 4.2. Here we only recall that the two-point functions are UV divergent and, in our case, where the internal lines are fermionic, IR finite.

THREE-POINT FUNCTION The three-point function C_0 is solved as well by introducing two Feynman parameters, x and y, which let the integral become proportional to

$$\int_0^1 \mathrm{d}x \int_0^x \mathrm{d}y\, [ax^2 + by^2 + cxy + dx + ey + f]^{-1}\,,$$

where the coefficients a, b, c, d, e and f depend on the arguments of the relevant C_0. At this stage, by particular shifts of y (see (58), section 5), one may get rid of x via a straightforward integration and obtains an integral expression like:

$$\int_0^1 \mathrm{d}y\, \frac{1}{P(y)} \log \frac{Q(y)}{Q(y_0)}\,,$$

where $P(y)$ and $Q(y)$ are a linear and a quadratic polynomial in y, respectively, and y_0 is a root of $P(y)$. This way of writing is convenient for the evaluation of the C_0 in terms of dilogarithms:

$$\mathrm{Li}_2(z) \equiv -\int_0^z \mathrm{d}t\, \frac{\log(1-t)}{t}\,.$$

In particular, it turns out that the most general three-point function may be written in terms of twelve dilogarithms.

Standard results in a cut-off regularization framework, compatible with our conventions, may be found in (62), appendix C. Here we only recall that the three-point functions are UV finite and, in our case, where at least one internal line is a photon propagator, IR divergent. The cases of our interest in which they are not IR divergent are highlighted in (59), section 3.3.

FOUR-POINT FUNCTION The four-point function D_0 is solved as well by introducing three Feynman parameters, but the computation is much more complicated and we only recall that, if the masses are real, one can in most cases construct equations giving the four-point function in terms of twenty-four dilogarithms. We refer the reader interested in the calculation to (58), section 6, while here we only quote eq. (2.13) from (62), since it solves our unique D_0 with two internal fermions and two internal photons, which showed up within the box contribution and whose IR divergence is regularized by a cut-off. Other standard results for the four-point functions may be found in (59), section 4.4, and (63).

BREMSSTRAHLUNG For sake of completeness we add to this appendix the evaluation of soft Bremsstrahlung integrals, namely phase-space integrals for photons with an energy less than some specified value. In particular the basic integral is:

$$\mathcal{I}(p_i, p_j) = \int^{k^0<\omega} \frac{\mathrm{d}^3\mathbf{k}}{k^0} \frac{1}{(p_i \cdot k)(p_j \cdot k)},$$

where $k = (k^0, \mathbf{k})$ is the Bremsstrahlung photon 4-momentum, $(k^0)^2 = \mathbf{k}^2 + \lambda^2$, ω is the maximum value of the photon energy and $p_{i,j} = (p^0_{i,j}, \mathbf{p}_{i,j})$ are two fermion 4-momenta.

The integrals with $p_i = p_j \equiv p$ yield a direct calculation:

$$\begin{aligned}
\mathcal{I}(p,p) &= \int^{k^0<\omega} \frac{\mathrm{d}^3\mathbf{k}}{k^0} \frac{1}{(p\cdot k)^2} \\
&= 2\pi \int_0^\omega \mathrm{dk} \frac{\mathrm{k}^2}{\sqrt{\mathrm{k}^2+\lambda^2}} \int_{-1}^1 \mathrm{dc}\, \frac{1}{m^2\gamma^2(\sqrt{\mathrm{k}^2+\lambda^2} - \beta \mathrm{kc})^2} \\
&= \frac{4\pi}{m^2\gamma^2} \int_0^\omega \mathrm{dk} \frac{\mathrm{k}^2}{\sqrt{\mathrm{k}^2+\lambda^2}[(1-\beta^2)\mathrm{k}^2+\lambda^2]} \\
&\simeq \frac{2\pi}{m^2}\left[2\log\frac{2\omega}{\lambda} - \frac{1}{\beta}\log\frac{1+\beta}{1-\beta}\right]
\end{aligned}$$

where m is the mass of the fermion, $\beta = |\mathbf{p}|/p^0$, $\gamma = 1/(1-\beta^2)^{1/2}$, $\mathrm{k} \equiv |\mathbf{k}|$ and $\mathrm{c} \equiv \cos\theta$, which shows up in the scalar product $p \cdot k$. The last equality holds in the limit $\lambda \to 0$, where $O(\lambda^2)$ terms may be

neglected.

In the other cases, when p_i is not a multiple of p_j, the procedure is more articulate and we follow (58), section 7. The trick is to introduce a parameter ρ such that:

$$(p-q)^2 = 0\,, \qquad p \equiv \rho p_i\,, \quad q \equiv p_j\,,$$

where the sign of $p_0 - q_0$ is the same of q_0. Thus, one introduces a Feynman parameter x by which the integration over $\mathbf{k}$ becomes straightforward. At this stage, we followed with our conventions the methods used in (58). As a result, also using dilogarithms and the limit $\lambda \to 0$, we eventually obtained:

$$\mathcal{I}(p_i, p_j) = -\frac{2\pi\rho}{v\ell}\Big[\frac{1}{2}\log\frac{p^2}{q^2}\log\Big(\frac{2\omega}{\lambda}\Big)^2 + \Big\{\frac{1}{4}\log^2\frac{u_0 - |\mathbf{u}|}{u_0 + |\mathbf{u}|} + \\ + \mathrm{Li}_2\Big(\frac{v + u_0 + |\mathbf{u}|}{v}\Big) + \mathrm{Li}_2\Big(\frac{v + u_0 - |\mathbf{u}|}{v}\Big)\Big\}_{u=q}^{u=p}\Big]\,,$$

where

$$\ell = p_0 - q_0\,, \qquad v = \frac{q^2 - p^2}{2\ell}\,.$$

In particular, in the center-of-mass frame, we shall have:

$$p_1^0 = p_2^0 = \sqrt{m^2 + \frac{\Lambda(s, m^2, M^2)}{4s}}\,, \quad |\mathbf{p_1}| = |\mathbf{p_2}| = \frac{\sqrt{\Lambda(s, m^2, M^2)}}{2\sqrt{s}}\,,$$
$$q_1^0 = q_2^0 = \sqrt{M^2 + \frac{\Lambda(s, m^2, M^2)}{4s}}\,, \quad |\mathbf{q_1}| = |\mathbf{q_2}| = \frac{\sqrt{\Lambda(s, m^2, M^2)}}{2\sqrt{s}}\,.$$

Hence, for our Bremsstrahlung integrals, the following hold:

- $\mathcal{I}(q_1, q_2)$:[1]

$$\rho_t = \frac{2M^2 - t + \sqrt{t^2 - 4tM^2}}{2M^2}\,,$$
$$\ell_t = \rho_t\, q_1^0 - q_2^0\,, \quad v_t = M^2\frac{1 - \rho_t^2}{2\ell_t}\,.$$

- $\mathcal{I}(q_1, p_1)$:

$$\rho_s = \frac{s - M^2 - m^2 + \sqrt{\Lambda(s, m^2, M^2)}}{2M^2}\,,$$
$$\ell_s = \rho_s\, q_1^0 - p_1^0\,, \quad v_s = \frac{m^2 - \rho_s^2 M^2}{2\ell_s}\,.$$

- $\mathcal{I}(q_1, p_2)$:

$$\rho_u = \frac{\sqrt{(s+t)^2 + (m-M)^2 - 2(s+t)(m^2+M^2)}}{2M^2} + \\ + \frac{m^2 + M^2 - s - t}{2M^2}\,, \quad \ell_u = \rho_u\, q_1^0 - p_2^0\,, \quad v_u = \frac{m^2 - \rho_u^2 M^2}{2\ell_u}\,.$$

1 The same holds for $\mathcal{I}(p_1, p_2)$, with $\{M, q_1, q_2\} \to \{m, p_1, p_2\}$.

BIBLIOGRAPHY

1. F. Jegerlehner, *The Anomalous Magnetic Moment of the Muon* (Springer International Publishing, 2017), vol. 274.
2. M. Knecht, "The Muon Anomalous Magnetic Moment", *Nucl. Part. Phys. Proc.* **258-259**, 235–240 (2015).
3. T. Aoyama, M. Hayakawa, T. Kinoshita, M. Nio, "Complete Tenth-Order QED Contribution to the Muon g-2", *Phys. Rev. Lett.* **109**, 111808 (2012).
4. K. Melnikov, A. Vainshtein, *The Anomalous Magnetic Moment of the Muon* (Springer-Verlag Berlin Heidelberg, 2006), vol. 216.
5. M. Passera, "The Standard model prediction of the muon anomalous magnetic moment", *J. Phys. G* **31**, R75–R94 (2005).
6. A. Czarnecki, W. J. Marciano, "The Muon anomalous magnetic moment: A Harbinger for 'new physics'", *Phys. Rev. D* **64**, 013014 (2001).
7. M. Della Morte, B. Jaeger, A. Juttner, H. Wittig, "Towards a precise lattice determination of the leading hadronic contribution to $(g-2)_\mu$", *JHEP* **03**, 055 (2012).
8. T. Blum *et al.*, "Connected and Leading Disconnected Hadronic Light-by-Light Contribution to the Muon Anomalous Magnetic Moment with a Physical Pion Mass", *Phys. Rev. Lett.* **118**, 022005 (2017).
9. C. C. Calame, M. Passera, L. Trentadue, G. Venanzoni, "A new approach to evaluate the leading hadronic corrections to the muon g-2", *Phys. Lett. B* **746**, 325–329 (2015).
10. G. Abbiendi *et al.*, "Measuring the leading hadronic contribution to the muon g-2 via μe scattering", *Eur. Phys. J. C* **77**, 139 (2017).
11. B. L. Roberts, *Nucl. Phys. Proc. Suppl.* **218**, 237 (2011).
12. H. Iinuma, *J. Phys. Conf. Ser.* **295**, 012032 (2011).
13. V. Shtabovenko, R. Mertig, F. Orellana, "New Developments in `FeynCalc` 9.0", *Comput. Phys. Commun.* **207**, 432–444 (2016).
14. R. Mertig, M. Boehm, A. Denner, "Feyn Calc - Computer-algebraic calculation of Feynman amplitudes", *Comput. Phys. Commun.* **64**, 345–359 (1991).
15. S. A. Goudschmidt, G. H. Uhlenbeck, "Spinning electrons and the structure of spectra", *Nature* **117**, 264–265 (1926).
16. E. Back, A. Landé, *Zeemaneffekt und Multiplettstruktur der Spektrallinien* (J. Springer, Berlin, 1925).

17. W. Pauli, "Zur Quantenmechanik des magnetischen Elektrons", *Zeits. Phys.* **43**, 601–623 (1927).

18. P. A. M. Dirac, "The Quantum Theory of the Electron", *Proc. Roy. Soc. A* **117**, 610–624 (1928).

19. L. E. Kinsler, W. V. Houston, "The Value of $\frac{e}{m}$ from the Zeeman Effect", *Phys. Rev.* **45**, 104–108 (1934).

20. P. Kusch, H. M. Foley, "The Magnetic Moment of the Electron", *Phys. Rev.* **74**, 250–263 (1948).

21. J. Schwinger, "On Quantum-Electrodynamics and the Magnetic Moment of the Electron", *Phys. Rev.* **73**, 416–417 (1948).

22. P. A. M. Dirac, "Does Conservation of Energy Hold in Atomic Processes?", *Nature* **137**, 298–299 (1936).

23. S. Eidelman, M. Passera, "Theory of the tau lepton anomalous magnetic moment", *Mod. Phys. Lett. A* **22**, 159–179 (2007).

24. C. M. Sommerfield, "Magnetic Dipole Moment of the Electron", *Phys. Rev.* **107**, 328–329 (1957).

25. A. Petermann, "Fourth order magnetic moment of the electron", *Helv. Phys. Acta* **30**, 407–408 (1957).

26. H. Elend, "On the anomalous magnetic moment of the muon", *Phys. Lett.* **20**, 682–684 (1966).

27. S. Laporta, "The Analytical value of the corner ladder graphs contribution to the electron (g-2) in QED", *Phys. Lett. B* **343**, 421–426 (1995).

28. S. Laporta, E. Remiddi, "The Analytical value of the electron (g-2) at order α^3 in QED", *Phys. Lett. B* **379**, 283–291 (1996).

29. S. Laporta, "The analytical contribution of the sixth-order graphs with vacuum polarization insertions to the muon (g-2) in QED", *Nuovo Cimento A (1965-1970)* **106**, 675–683 (1993).

30. S. Laporta, E. Remiddi, "The analytical value of the electron light-light graphs contribution to the muon (g-2) in QED", *Phys. Lett. B* **301**, 440–446 (1993).

31. A. Czarnecki, M. Skrzypek, "The muon anomalous magnetic moment in QED: three-loop electron and tau contributions", *Phys. Lett. B* **449**, 354–360 (1999).

32. A. Kurz *et al.*, "Electron contribution to the muon anomalous magnetic moment at four loops", *Phys. Rev. D* **93**, 053017 (2016).

33. S. Laporta, "High-precision calculation of the 4-loop contribution to the electron g-2 in QED", *Phys. Lett. B* **772**, 232–238 (2017).

34. P. J. Mohr, B. N. Taylor, D. B. Newell, "CODATA recommended values of the fundamental physical constants: 2010", *Rev. Mod. Phys.* **84**, 1527–1605 (2012).

35. R. Jackiw, S. Weinberg, "Weak-Interaction Corrections to the Muon Magnetic Moment and to Muonic-Atom Energy Levels", *Phys. Rev. D* **5**, 2396–2398 (1972).

36. I. Bars, M. Yoshimura, "Muon Magnetic Moment in a Finite Theory of Weak and Electromagnetic Interactions", *Phys. Rev. D* **6**, 374–376 (1972).

37. G. Altarelli, N. Cabibbo, L. Maiani, "The Drell-Hearn sum rule and the lepton magnetic moment in the Weinberg model of weak and electromagnetic interactions", *Phys. Lett. B* **40**, 415–419 (1972).

38. W. Bardeen, R. Gastmans, B. Lautrup, "Static quantities in Weinberg's model of weak and electromagnetic interactions", *Nuc. Phys. B* **46**, 319–331 (1972).

39. K. Fujikawa, B. W. Lee, A. I. Sanda, "Generalized Renormalizable Gauge Formulation of Spontaneously Broken Gauge Theories", *Phys. Rev. D* **6**, 2923–2943 (1972).

40. A. Czarnecki, W. J. Marciano, A. Vainshtein, "Refinements in electroweak contributions to the muon anomalous magnetic moment", *Phys. Rev. D* **67**, 073006 (2003).

41. A. Czarnecki, B. Krause, W. J. Marciano, "Electroweak Fermion loop contributions to the muon anomalous magnetic moment", *Phys. Rev. D* **52**, R2619–R2623 (1995).

42. C. Gnendiger, D. Stöckinger, H. Stöckinger-Kim, "The electroweak contributions to $(g-2)_\mu$ after the Higgs boson mass measurement", *Phys. Rev. D* **88**, 053005 (2013).

43. G. Degrassi, G. F. Giudice, "QED logarithms in the electroweak corrections to the muon anomalous magnetic moment", *Phys. Rev. D* **58**, 053007 (1998).

44. C. Bouchiat, L. Michel, "La résonance dans la diffusion méson π-méson π et le moment magnétique anormal du méson μ", *J. Phys. Radium* **22**, 121 (1961).

45. K. Hagiwara, R. Liao, A. D. Martin, D. Nomura, T. Teubner, "$(g-2)_\mu$ and $\alpha(M_Z^2)$ re-evaluated using new precise data", *J. Phys. G* **38**, 085003 (2011).

46. F. Jegerlehner, R. Szafron, "$\rho_0 - \gamma$ mixing in the neutral channel pion form factor $F_\pi^{(e)}(s)$ and its role in comparing e^+e^- with τ spectral functions", *Eur. Phys. J. C* **71**, 1632 (2011).

47. M. Davier, A. Hoecker, B. Malaescu, Z. Zhang, "Reevaluation of the hadronic contributions to the muon $g-2$ and to $\alpha(M_Z^2)$", *Eur. Phys. J. C* **71**, 1515 (2011).

48. K. Melnikov, A. Vainshtein, "Hadronic light-by-light scattering contribution to the muon anomalous magnetic moment reexamined", *Phys. Rev. D* **70**, 113006 (2004).

49. G. W. Bennett *et al.*, "Measurement of the Negative Muon Anomalous Magnetic Moment to 0.7 ppm", *Phys. Rev. Lett.* **92**, 161802 (2004).

50. G. W. Bennett *et al.*, "Final report of the E821 muon anomalous magnetic moment measurement at BNL", *Phys. Rev. D* **73**, 072003 (2006).

51. A. Nikishov, "Radiative corrections to the scattering of μ mesons on electrons", *Sov. Phys JETP* **12**, 529–535 (1961).

52. K. E. Eriksson, "Radiative corrections to muon-electron scattering", *Nuovo Cimento* **19**, 1029–1043 (1961).

53. K. E. Eriksson, B. Larsson, G. A. Rinander, "Radiative corrections to muon-electron scattering", *Nuovo Cimento* **30**, 1434–1444 (1963).

54. P. van Nieuwenhuizen, "Muon-electron scattering cross section to order α^3", *Nuc. Phys. B* **28**, 429–454 (1971).

55. T. V. Kukhto, N. M. Shumeiko, S. I. Timoshin, "Radiative corrections in polarised electron-muon elastic scattering", *J. Phys. G* **13**, 725 (1987).

56. D. Yu. Bardin, L. Kalinovskaya, "QED corrections for polarized elastic muon e scattering", arXiv: `hep-ph/9712310` (1997).

57. N. Kaiser, "Radiative corrections to lepton-lepton scattering revisited", *J. Phys. G* **37**, 115005 (2010).

58. G. 'tHooft, M. Veltman, "Scalar one-loop integrals", *Nucl. Phys. B* **153**, 365–401 (1979).

59. R. K. Ellis, G. Zanderighi, "Scalar one-loop integrals for QCD", *JHEP* **02**, arXiv: `0712.1851 (hep-ph)` (2008).

60. P. Mastrolia, M. Passera, A. Primo, U. Schubert, "Master integrals for the NNLO virtual corrections to μe scattering in QED: the planar graphs", arXiv: `1709.07435 (hep-ph)` (2017).

61. G. Passarino, M. Veltman, "One-loop corrections for e^+e^- into $\mu^+\mu^-$ in the Weinberg model", *Nucl. Phys. B* **160**, 151–207 (1979).

62. W. Beenakker, A. Denner, "Infrared divergent scalar box integrals with applications in the electroweak standard model", *Nucl. Phys. B* **338**, 349–370 (1990).

63. A. Denner, S. Dittmaier, "Scalar one-loop 4-point integrals", *Nucl. Phys. B* **844**, 199–242 (2011).

64. J. Ellis, "TikZ-Feynman: Feynman diagrams with TikZ", *Comput. Phys. Commun.* **210**, 103–123 (2017).

COLOPHON

This document was typeset using the typographical look-and-feel `classicthesis` developed by André Miede. The style was inspired by Robert Bringhurst's seminal book on typography "*The Elements of Typographic Style*". `classicthesis` is available for both LaTeX and LyX:

https://bitbucket.org/amiede/classicthesis/

Ti*k*Z-Feynman (*64*) was used to draw Feynman diagrams.